| | Doc.nr: | CATO2-WP3.04-D16 |
| --- | --- | --- |
| | Version: | 2013.12.19 |
| | Classification: | Public |
| | Page: | 1 of 42 |

**Corrosion monitoring**

# CATO-2 Deliverable WP3.4-D16
## Specifications and design criteria for innovative corrosion monitoring and (downhole) sensor systems, including sensitivity analysis

| Prepared by: | Xiaolong Zhang (TNO)<br>Efe Kermen (WEP) |
| --- | --- |
| Reviewed by: | Jens Wollenweber, Manuel Nepveu (both TNO) |
| Approved by: | J.Brouwer<br>(CATO-2 Director) |

# 1 Executive Summary (restricted)

This report focuses on the corrosion monitoring and corrosion sensor systems, for use in $CO_2$ storage wells, including a sensitivity analysis. The feasibility for using new sensors to measure well integrity based on electrochemical principles is investigated.

The use of corrosion sensors in $CO_2$ storage wells is at its infancy. The application of tools based on mechanical, sonic, electromagnetic, and optical principles has a limitation of sensitivity. They hardly detect pinholes in the tubing. Electrochemical sensors have been used in the oil industry, but little experience has been documented with respect to usage in $CO_2$ storage wells.

This work focusses on investigating electrochemical sensors to monitor the corrosion of the casing in $CO_2$ storage wells. Corrosion of steels in $CO_2$ environments, materials selection and corrosion monitoring tools are surveyed in this report

The casing steel N80 and Cr13 steel have been studied using electrochemical measurements in autoclaves. The well P18 in the North Sea has been chosen as an example epresentative for environmental conditions. The corrosion rates of steels have been studied in brine plus $CO_2$ and $H_2S$ at different pressures and temperatures. Corrosion monitoring sensors based on electrochemical measurements (principles?) have been designed and characterized in different conditions. The sensitivity of the sensors has also been analysed.

The main results on the sensors are as follows:

1) The corrosion sensors can measure corrosion resistance (and corrosion rate) of casing steel N80 downhole using LPR, EIS and ENM techniques. All three modes reflect the corrosion level of the casing steel although they give different values. The LPR and EIS modes also reflect pressure changes downhole. The ENM mode is good for long term monitoring and the other two modes are suitable for routine checking of the corrosion status of the tubing materials time by time.

2) The corrosion sensors are sensitive to environmental electromagnetic disturbances and the probe systems have to be well shielded from these for reliable measurements.

3) LPR is not suitable for stainless steel that is susceptible to pitting and not uniform corrosion.

4) The stainless steel probe needs further scrutiny as the prediction of localized corrosion is difficult.

# Distribution List

(This section shows the initial distribution list)

| External | Copies | Internal | Copies |
|---|---|---|---|
|  |  |  |  |
|  |  |  |  |

# Document Change Record

(This section shows the historical versions, with a short description of the updates)

| Version | Nr of pages | Short description of change | Pages |
|---|---|---|---|
|  |  |  |  |
|  |  |  |  |

# Table of Content

# 2 Applicable/Reference documents and Abbreviations

## 2.1 Applicable Documents

(Applicable Documents, including their version, are documents that are the "legal" basis to the work performed)

|  | Title | Doc nr | Version |
|---|---|---|---|
| AD-01d | Toezegging CATO-2b | FES10036GXDU | 2010.08.05 |
| AD-01f | Besluit wijziging project CATO2b | FES1003AQ1FU | 2010.09.21 |
| AD-02a | Consortium Agreement | CATO-2-CA | 2009.09.07 |
| AD-02b | CATO-2 Consortium Agreement | CATO-2-CA | 2010.09.09 |
| AD-03g | Program Plan 2013b | CATO2-WP0.A-D03 | 2013.04.01 |
|  |  |  |  |

## Reference Documents

(Reference Documents are referred to in the document)

|  | Title | Doc nr | Version/issue | Date |
|---|---|---|---|---|
| none |  |  |  |  |
|  |  |  |  |  |
|  |  |  |  |  |

## Abbreviations

(This refers to abbreviations used in this document)

| | |
|---|---|
| API | American Petroleum Institute |
| DCMS | Downhole corrosion monitoring system |
| EDS | Extensive expersive spectroscopy |
| EIS | Electrochemical impedance spectroscopy |
| ENM | Electrochemical noise measurement |
| LPR | Linear polarization resistance |
| OCP | Open circuit potential |
| SEM | Scanning electronic microscopy |
| XRD | X-ray diffraction |
|  |  |

# 3    CO$_2$ Corrosion

## 3.1    Corrosion mechanism

Dry $CO_2$ is not corrosive, however $CO_2$ in combination with water creates an acidic environment that causes corrosion of steels.  Corrosion process includes the following reactions:

$$CO_2 + H_2O \rightarrow H^+ + HCO_3^-$$
$$2(H^+ + HCO_3^-) + Fe \rightarrow Fe^{2+} + 2HCO_3^- + H_2$$
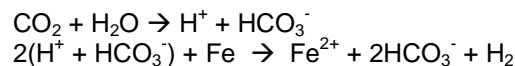
At the steel/liquid interface, an anodic reaction takes place and iron atoms are oxidized as cations. At the meantime, a cathodic reaction takes place and protons are reduced. Bicarbonate and carbonate anions can react with ferrous ions to form an iron carbonate film.
Downhole corrosion of casing steel and tubes affects the integrity of the $CO_2$ storage system.The corrosion rate of casing steel depends on various variables: pressure, temperature, the presence and quality of well cement, salts and chemicals in the brine, pH etc.(Choi et al., 2013, 2010; Dugstad et al., 2011; Pfennig and Bäßler, 2009; Seiersten and Kongshaug, 2005; Seiersten, 2001; Zhang et al., 2013). So far limited data are available for casing steel corrosion in $CO_2$ storage.

## 3.2    Corrosion controlling factors

$CO_2$ corrosion depends on the following factors:
- Presence of water; an oil-wet system protects steel from corrosion.
- $CO_2$-content; if the partial pressure exceeds 2 bar, corrosion occurs significantly in a water wet environment.  (Partial pressure = total pressure x volume fraction of $CO_2$ gas component).
- $H_2S$-content; even in low concentrations in combination with $CO_2$, this mixture can cause severe corrosion, particularly leading to sulphide stress cracking.
- Oxygen content and content of other oxidising agents.
- Temperature; when over 150 °C, a dramatic increase in corrosion rate occurs.
- Pressure; generally the corrosive reaction accelerates with increasing pressure.
- pH.
- Chloride concentration; chloride enhances corrosion.
Condensing conditions; if water drops out of the gas stream, corrosion will occur.

In Carbon Sequestration, $CO_2$ is usually injected into the formation in supercritical state. The corrosion risk is low under such circumstances because the corrosion rate of metals in presence of dry supercritical $CO_2$ is very low. However, the rate of corrosion will increase if the injected stream comes into contact with water. Possible water sources under these conditions are the connate water in the injection zone, free water in the cement or free water resulting from capillary condensation (Kolenberg et al., 2012).
After the injection period, during the long-term storage phase, the supercritical $CO_2$ can be hydrated with water present in the reservoir and wet $CO_2$ and the resulting acid brine can reach the well. Then acidic water can degrade the cement protecting the steel casing.

| | Doc.nr: | CATO2-WP3.04-D16 |
| --- | --- | --- |
| | Version: | 2013.12.19 |
| | Classification: | Public |
| | Page: | 7 of 42 |

**Corrosion monitoring**

# 4 Corrosion in Different Wells

Assuming that the injected $CO_2$ is successfully confined in the target formation, $CO_2$ corrosion will likely occur in all  wells; $CO_2$ injection well(s) that inject $CO_2$ into the target formation, monitoring wells that penetrate the target formation (most likely converted from a suspended/active well) and previously abandoned wells. Different types of wells have different designs and configurations. The occurrence of $CO_2$ corrosion will differ with these..

## *4.1   CO<sub>2</sub> injection well*

These wells will come into contact with $CO_2$ more intensively than any other well. Even though $CO_2$ will be mostly injected in the supercritical state, injection wells are still the most susceptible to corrosion. Moreover, high pressures necessary for injection means that the corrosion rate will also be the highest. For these reasons and because of the delicacy of Carbon Sequestration (especially on the environmental aspect), EPA has defined a new category of wells and sets of regulations for $CO_2$ injection wells in the United States. These so-called Class VI wells are designed not only for the injection of the $CO_2$, but are built to survive the whole duration of the geological sequestration project in question (USEPA, 2012).

Two common configurations of an injection well are displayed on the figure below (Figure 4-1). The $CO_2$ is injected from the surface through injection tubing, which is a small diameter pipe string running from the wellhead to the target reservoir. The injected $CO_2$ disperses into the target formations either through well screens installed at the end of the tubing or through perforations on the liner. If a liner is present in the injection zone, it will be cemented to ensure that the integrity of the inner casing is maintained. However, cemented liners are not preferred as the excess water in cement will act as a medium that will enhance corrosion in the injection zone.

In an environment where dry supercritical $CO_2$ is injected, $CO_2$ corrosion will not take place through the injection tubing, unless condensation occurs deeper into the well. However, corrosion will definitely take place in the injection zone, where the injected substance will come into contact with water. Therefore it is important to limit the corrosion to the injection zone, and minimize its effects for well integrity reasons,.

The injection zone is isolated from the wellbore by a packer installed just above the target formation. A packer is a device that can be run into a wellbore with a smaller initial outside diameter. When the packer is activated, the sealing elements expand toward the inner casing, and seal the casing-tubing annulus. The packer keeps fluid from migrating from the injection zone into the annulus between the long-string casing and tubing. The sealing element of the packer is an elastomer, such as nitrile rubber. Packers can be nickel plated especially in HPHT environments to protect the integrity of the elastomer. The packer is an important device for internal well integrity. It is essential that the packer material is compatible with any fluid that it will come in contact with; in our case these fluids will be wet $CO_2$ below, and completion fluid above. Packers have a life expectancy of 10-20 years, and must be renewed regularly in order to maintain integrity.
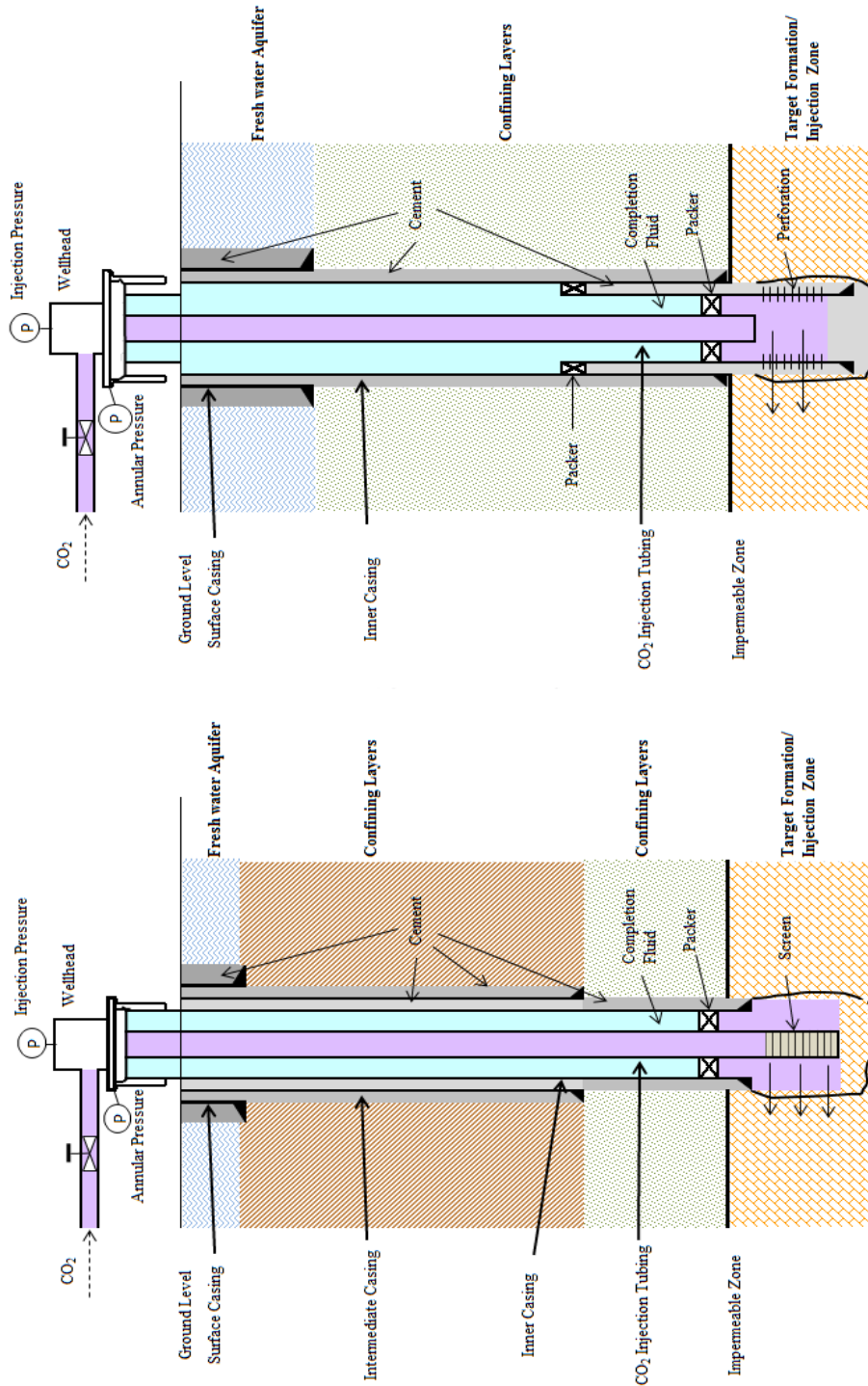
**Figure 4-1.** Example well schematics for $CO_2$ injection wells.

| | |
| --- | --- |
| Doc.nr: | CATO2-WP3.04-D16 |
| Version: | 2013.12.19 |
| Classification: | Public |
| Page: | 9 of 42 |

**Corrosion monitoring**

In an injection well, the annular space between the inner casing and injection tubing above the packer is filled with a completion fluid. This fluid is ideally non-corrosive, and serves as a protection for the casing against $CO_2$ that might leak through the packer or injection tubing. To ensure that the $CO_2$ seeping through a potential leak does not come into contact with the casing or the wellhead, the annular pressure must be higher than the injection pressure. With a higher annular pressure, the injected $CO_2$ would not be able to escape into the annular. Instead, the annular fluid will flow into the zone where the integrity is lost, because of the pressure difference. All pipe strings in the well except the innermost string is called casing. A single injection well may have two or more different casing sizes. The number of casing strings in a well is based on design criteria and target specifications. The casing string that is most susceptible to $CO_2$ corrosion is the string encircling the injection tubing, as parts are in direct contact with the injected fluid and formation water. The chance of $CO_2$ corrosion from the injection zone becomes minimal for surface casing and any intermediate casing strings (if present).

Cementing casing strings is a common practice in the oil field. In a $CO_2$ injection well, each casing string is cemented from the shoe (bottom of the casing) to the surface to minimize pore space and the chance of fluid migration. If a liner is present, it is cemented to the shoe of the previous casing string. As wet $CO_2$ is also corrosive to cement, it is important to pick a cement type that is more durable in $CO_2$ environments. Nevertheless, it is important to point out that failing to cement the casing over its entire length, failure of the cement to bond with the casing or formation, not centralizing the casing during cementing, cracking, and alteration of the cement all can allow migration of fluids along the well bore.

Regardless of the well configuration (whether it is casing or a liner), the bottom part of this inner string will be inside the injection zone, and will most definitely come into contact with wet $CO_2$. To maintain the integrity of the injection well throughout the project, it is significant to monitor the corrosion taking place at this interval, and take necessary actions to prevent the leakage of corrosive fluid outside the injection zone.

## 4.3    Monitoring wells

Monitoring wells form an essential part of the CCS network. As the name suggests, these wells are used to monitor the injection and storage of the $CO_2$. These wells are mainly used to assess injection performance and confirm successful confinement of the injected $CO_2$. Since exposure to $CO_2$ is not the primary concern with these wells, these wells are usually not constructed as robust as injection wells. Most monitoring wells will not penetrate into the target formation in order to minimize the possibility of a leak. These wells will most probably be completed with standard casing/tubing (K55 or N80) that is susceptible to $CO_2$ corrosion. They might even have open hole completions. In such wells, the integrity of the well is kept by cementing the inner tubing/casing to surface, and placing a bentonite seal above the screened interval, while monitoring is carried with tools lowered into the screened interval. Depending on the methods applied, the inner casing/tubing may or may not be filled with fluids.

More measures need to be taken against potential corrosion if the monitoring well in fact penetrates the injection zone. Most of these wells would have been active or suspended wells that have been used for production/injection of material from the same formation. These wells may or may not be designed for $CO_2$ environment, and material susceptible for $CO_2$ may have been used in the completion (Although, regulations of the governing body will probably dictate that the completion should be renewed accordingly).  If the well is designed for monitoring Carbon Sequestration, the innermost tubing/casing will be made from corrosion resistant material, and a packer will be set at the inner casing shoe above the screened interval to contain the $CO_2$ in the lower parts of the well (Figure 4-2). The annulus below the packer is usually filled with sand or gravel packs. Designed to prevent the flow of formation particles into the inner tubing/casing, these packs are also placed in wells that do not penetrate the injection zone.
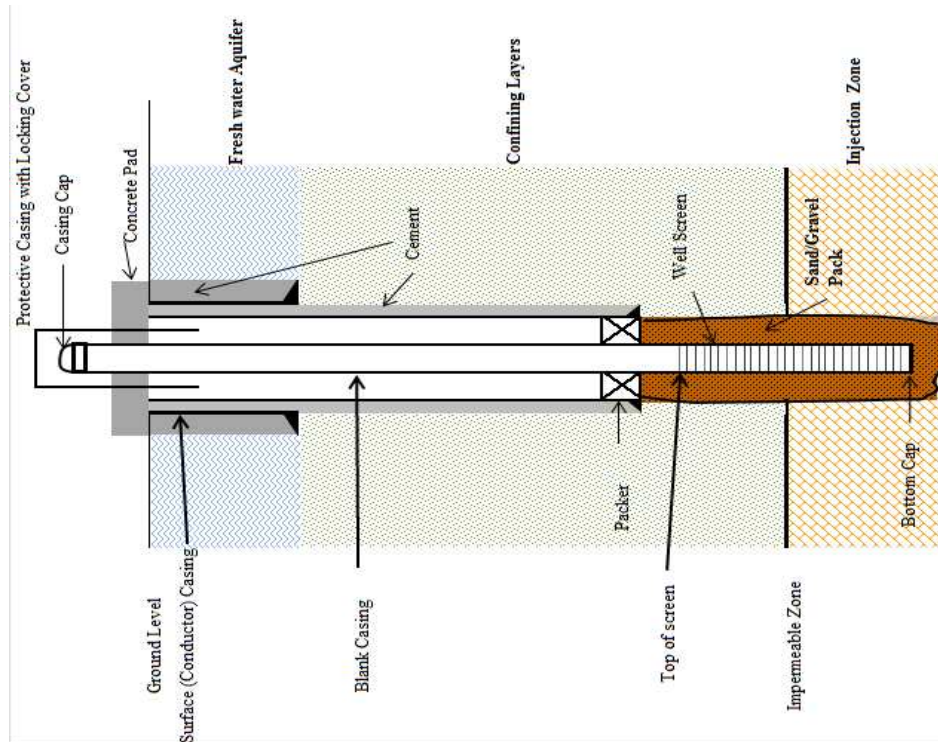
**Figure 4-2**. Schematic of a monitoring well that penetrates the injection zone.

## 4.4   Abandoned wells

Abandoned wells are considered as the biggest integrity issue in CCS projects. They have fulfilled their purpose and have been closed and secured in a way that maintains the integrity of the hole and the formations surrounding it. The main concerns about abandonment are the difficulties in confirming the quality of abandonment, and potentially sub-standard material use during abandonment. As the well in question may have been abandoned decades ago, it would be nearly impossible to gather data about the well and the abandonment process. Furthermore, due to lower industry standards in the past, the material used in the well and the abandonment process may be of lower quality and more susceptible to $CO_2$ corrosion.

To abandon a well, all casing that extends to the surface is cut to a certain depth (3 meters onshore, 6 m offshore in the Netherlands) and a surface cement plug that extends at least 100 m will be placed on the top of the well. Alternatively a shorter cement plug can be placed in combination with a mechanical plug placed below the cement. Moreover, additional barriers are installed around the lowermost casing and above the production/injection zone to prevent the flow of formation fluid into the well (Kermen and Meekes, 2013). These can be mechanical, cement or a combination of the two. It is also a common practice to fill the uncemented portions of the abandoned well with bentonite or drilling mud.
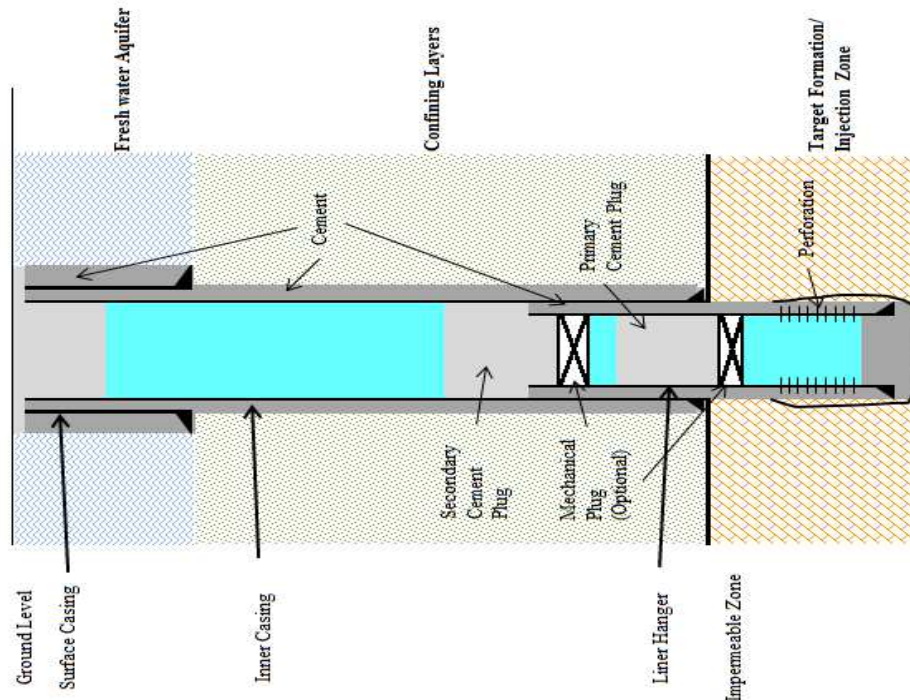
| | Doc.nr: | CATO2-WP3.04-D16 |
| :--- | :--- | :--- |
| | Version: | 2013.12.19 |
| | Classification: | Public |
| | Page: | 11 of 42 |

**Corrosion monitoring**



**Figure 4-3.** Schematic of an abandoned well

In the past a well was abandoned solely for the purpose of ending any activities regarding the well. Any potential future use of the well was not taken into consideration during abandonment. Therefore, no measures would be taken against potential downhole corrosion, unless the zone in question contained corrosive fluids. In such conditions (and if the regulations allowed it at the time of abandonment), the primary and secondary barriers (downhole plugs) may not contain any cement. This would create problems in corrosive $CO_2$ environments, as the plugs can corrode very quickly. Furthermore, casing and tubing material in such an abandoned well is also unlikely to be corrosion resistant unless enforced by regulating bodies.

Monitoring downhole corrosion directly is not possible unless access into the wellbore is regained. This is a very costly operation, and it will not be exercised unless serious concerns over the integrity of the well in question exist or it has been confirmed that the well integrity has been compromised.

## *4.5 Reservoir properties*

The reservoir characteristics are important to determine the corrosion potential in a well. Higher pressures and temperatures increase the rate of corrosion. Downhole temperature conditions are influenced by two parameters; the surface temperature and the depth of the target formation. The temperature gradient in the Netherlands is about 0.030 – 0.035°C/m TVD. Depending on the depth of the target, downhole temperature can be as low as 50°C, and as high as (or maybe higher than) 150°C.

Determining the injection pressure is a more complex matter. In order to inject $CO_2$ into the target formation, the injection pressure must exceed the pore pressure of the reservoir. In a non-depleted field, the pore pressure gradient is about 0.1 bar/m. If these are satisfied, injection pressures of over 200 bars will be required to successfully inject $CO_2$. However, if the target

formation is a previously depleted reservoir, significantly lower injection pressures would suffice. The maximum allowable injection pressure should also be limited in a Carbon Sequestration Project. In EPA's Class VI Well Injection Guidance document, it is stated that the injection pressure should not exceed 90% of the reservoir fracturing pressure. Unless hydraulic stimulation is intended, fracturing the injection zone should not be practiced as it can create uncontrolled $CO_2$ leaks which would endanger the entire project(USEPA, 2012).

Some $CO_2$ injection sites and their operating pressures are listed below(Nagelhout et al., 2009).

- Weyburn $CO_2$ EOR; 150 bar (2175 psi)
- SACROC $CO_2$ EOR; 138 bar (2000 psi)
- Lacq pilot CCS project; 70-80 bar (unconfirmed; reservoir pore pressure 30-80 bar at 4500 m)
- In Salah pilot CCS project; 279 bar (estimated injection pressure after three years)
- Ketzin; maximum 85 bar at 550 m.

# 5    Well Construction Materials in Wet CO$_2$ Environments

Material selection for Carbon Sequestration wells depends on several factors like high strength requirements combined with high corrosion resistance of the material. A chemical analysis of the reservoir fluids is generally required for evaluation of the corrosive components such as hydrogen sulphide, carbon dioxide and chlorides. The presence of these components in the target formation will enhance the corrosion on well equipment significantly. Other components like temperature profile, pressure profile and stresses on the tubulars have also to be considered. When assessing wells or selecting materials for Carbon Sequestration, one has to consider that the wells will be in contact with wet CO$_2$, in particular in the deeper section.

## 5.1    Steel types

Some steel types used for well construction are listed below, with increasing corrosion resistance;

- **Carbon steel:** Contain less than 2.1% carbon in their chemical composition. Most commonly used, standard steel grades such as; K55, N/L80, P110 are amongst carbon steel pipes. K55 and N80 are the most basic steel grades with no additional corrosion resistant material present in their composition. Furthermore, any heat treatment on these grades of tubulars is optional. Other carbon steel grades such as L80 and P110 contain corrosion resistant material such as Manganese and Nickel, and undergo some form of heat treatment during the manufacturing phase. Tubuluars of this grade are extremely vulnerable to corrosion. K55 grade carbon steel casing is often used as surface casing, while L80 is the most commonly used casing material in the Netherlands under normal circumstances.

- **Martensitic stainless / corrosion resistant steel:** Contains at least 11.5% chromium such as Cr13 & Cr17 steel. Most wells in the Netherlands are completed with Cr13 tubing. Martensitic steels are not very corrosion resistant and are susceptible to sulphide stress cracking, which makes them ineffective in H$_2$S environments. On the other hand, they are extremely resistant to chloride stress cracking (CSC).

- **Super martensitic stainless steel:** Contains less carbon and more nickel and molybdenum, and is more resistant to corrosion than normal martensitic Cr13 steel. An example is Super Cr13 from V & M. According to SINTEF report on well integrity during CO$_2$ injection, Super Cr13 is 5 times to 44 times more resistant to corrosion than Cr13 depending on the temperature and pressure conditions (2007).

- **Ferritic-austenitic steel alloy**: Also known as duplex steel, this type of steel contains chromium, manganese, nickel, vanadium and molybdenum. As the name suggests, it is a mixture of austenitic and ferritic steel. It is much stronger than austenitic steel, and is also more resistive to corrosion pitting and stress cracking than regular austenitic steel. The overall corrosion resistance is also better than that of regular austenitic steel. They are characterised by low carbon content, high chromium (at least 20%) and molybdenum content (3-5%), and low nickel content (less than 5%) compared to austenitic steel. Cr22 is the most frequently used duplex steel in the oil industry. Superduplex steel (Cr25) contains significantly more nickel and molybdenum.

- **Austenitic / superaustenitic steel alloys:** These consist mostly of nickel and cobalt alloys. Austenitic steels contain at least 16% chromium and 10% nickel – manganese combination. Common austenitic steels such as CrNi18-9 or CrNiMo17-12-2 only provide average corrosion resistance. Furthermore, these materials are fairly susceptible to stress cracking caused by both sulphides and chlorides. On the other hand super-

austenitic steel alloys are resistant to stress cracking and provide very high overall corrosion resistance. Superaustenitic steel alloys contain very high (+30%) amounts of nickel and high molybdenum content (+6%) to protect from chloride pitting and crevice corrosion.   Alloys such as Inconel 625, Hastelloy C-22 and Hastelloy C-276 are amongst superaustenitic material.

Table 5-1:The table below summarizes characteristics of prospective materials for tubulars.

| Some Prospective Alloys for Hot Well Tubulars | | | | | | |
|---|---|---|---|---|---|---|
| | Major Alloying Constituents, wt% | | | General Corrosion | Cracking Resistance | |
| Alloy | Cr | Ni | Mo | Resistance[1] | SSC | CSC |
| CrNi18-9 | 18-20 | 8-10.5 | - | F | S | S |
| CrNiMo17-12-2 | 16-18 | 10-14 | 2-3 | F | S | S |
| Cr13 | 11.5-13.5 | 0.75 | - | S | S | R |
| Cr17 | 16-18 | 0.75 | - | F | S | R |
| Super Cr13 | 11.5-13.5 | 5 | 2 | F | F | R |
| Duplex SS (Cr 22) | 22 | 5 | 3 | G | S | G |
| Superduplex (Cr | 25 | 7 | 4 | G | G | G |
| 25) | 21.5 | 42 | 3 | G | R | R |
| Incoloy 825 | 21.5 | min. 58 | 9 | R | R | R |
| Inconel 625 | 22 | 26 | 5 | G | R | R |
| Haynes 20 Mod | 22 | 56 | 13 | R | R | R |
| Hastelloy C-22 | 16 | 57 | 16 | R | R | R |
| Hastelloy C-276 | 20 | 35 | 2.5 | G | R | R |
| Carpenter 20 Cb | | | | | | |
| SS = Stainless / Corrosion Resistant Steel | | | | G = Good<br>F  = Fair<br>S  = Susceptible<br>R  = Resistant | | |

## 5.2   Corrosion resistant alloys (CRA)

Corrosion resistant alloys have been divided into groups 1,2,3,4 based on their technical specifications,. It should be noted that there are no industry standards for Group 2-4 alloys. API 5CT, the only existing standard for well construction material, only covers 13Cr steel, which is a grade in Group 1.

**Group-1: Martensitic and Martensitic-Ferritic Stainless Steel**

Martensitic and Martensitic-Ferritic stainless steel alloy are the simplest corrosion resistant alloys. They are the most commonly used corrosion material resistant in the oil industry. Group 1 alloys are available for the yield strength range of 80-110 kpsi.

- **Chemical composition:**

  Sulphur content should be kept as low as possible. With a sulphur content of 0.001% the hot workability is equivalent to that of carbon steel. This requirement is essential when working upset pipes. A value of 0.004% max. is realistic.

- **Heat treatment:**

  One of the main advantages of 13Cr steel is its strength, which is obtained through austenizing and tempering. Tubulars are generally austenized at about 980 °C and because of its excellent hardenability they are air cooled which results in a fully

| | Doc.nr: | CATO2-WP3.04-D16 |
|---|---|---|
| | Version: | 2013.12.19 |
| | Classification: | Public |
| | Page: | 15 of 42 |

**Corrosion monitoring**

martensitic structure. Tempering temperature is about 710 °C. NACE Standard MR-01-75 requires double tempering for all martensitic stainless steels when used in sour environments, but there is no evidence that the double tempering improves the material resistance to $H_2S$ environments. Pipe manufacturers usually apply only one tempering.

- **Microstructure checks:**
  The only requirements for microstructures are related to delta ferrite content that shall not exceed 5% and microstructures are required to have grain boundaries with no continuous precipitates.

- **Hardness:**
  The NACE MR-01-75 suggested limit of 22 HRC for the 80 kpsi minimum yield strength, is a difficult task for Cr13 due to its high yield-to-tensile-ratio. As suggested by API 5 CT a more realistic value is 23 HRC.

- **Impact Properties:**
  The impact properties at low temperatures should be determined. Suggested test temperature is -10° C. In case the minimum service temperature is less than -10 °C, the test temperature should be agreed with the manufacturer.

### Group 2: Duplex Stainless Steel

Duplex stainless steel offers several advantages over martensitic alloys. The duplex grades have higher resistance to chloride stress corrosion cracking and also have good crevice and pitting corrosion resistance. They are available in a wide yield strength range from 65 kpsi up to 140 kpsi. As mentioned before, there is no standard that covers such materials to date, therefore the following features need to be carefully evaluated:

- **Chemical composition:**
  In general it is recommended to be at the high end of the range for chromium and molybdenum, while the sulphur content should be kept as low as possible.

- **Heat treatment:**
  Depending on the final size, during manufacturing pipes may undergo a solution annealing treatment either after heat extrusion or between the intermediate and final cold working phases. The scope of the heat treatment is to obtain the best microstructure while maintaining carbides in solid solution and to relieve all stresses. This is achieved by heating to allow the carbon to come into solution followed by rapid cooling to keep carbon in solution. For the optimal stabilisation of ferritic and austenitic phases the material needs to receive a direct quenching after heat treatment.

- **Hardness:**
  The NACE MR-01-75 limit of 28 HRC for the solution annealed condition is acceptable. The limit of 36 HRC for the high-strength cold worked condition is not achievable for the 125/140 grades. A more realistic value is 37/38 HRC.

- **Microstructure checks:**
  The microstructure shall have a ferritic-austenitic structure. The microstructure is required to have grain boundaries with no continuous precipitates. Intermetallic phases, nitrides and carbides shall not exceed 1.0%. Typically the ferrite volume fraction shall be in the range 40% to 60% for duplex and in the range 35% to 55% super duplex.

- **Impact Properties:**
  The impact properties at low temperatures should be determined. Suggested test temperature is -10° C. In case the minimum service temperature is less than -10 ° C, the test temperature should be agreed with the manufacturer.

**cato₂**

Doc.nr:          CATO2-WP3.04-D16
Version:         2013.12.19
Classification:  Public
Page:            16 of 42

**Corrosion monitoring**

For **Group 3 and 4 alloys**, the amount of alloying increases up to eight times more nickel and three times more molybdenum while maintaining about the same chromium content. Group 3 and 4 alloys are chosen for improved corrosion resistance to $H_2S$, $CO_2$ and chlorides. The chemistry of these alloys is very important. For the microstructures, evaluate the absence of carbide precipitates at grain boundaries that can compromise the corrosion resistance. Intermetallic phases, nitrides and carbides should not exceed 1.0%.

In addition to chemical and metallurgical evaluations, corrosion testing is also recommended to verify that the materials will meet the expected performance. The specification should include accelerated corrosion tests because testing in standard condition would take several months. The Slow Strain Rate Tensile Test (SSRT) is a test that can usually be requested because of its short duration. The standard test conditions are: 148.9°C (300°F), 6.9 bar (100 psi) $H_2S$ partial pressure at ambient pressure and temperature, 25% NaCl brine and 0.5% acetic acid(Cerruti, 1998).

## 5.3    Material selection

The choice of material for $CO_2$ injection wells will largely depend on the temperature and to a lesser degree on pressure conditions that are expected for the well and the presence of other corrosive agents, in particular $H_2S$ and water. Furthermore it is important not to mix low grade metal seals with high grade tubing/casing metal. This will lead to galvanic corrosion due to the difference in electric potential between the metals.

For injecting more than 95% pure $CO_2$ in wells, the following guidelines can be used for material selection:

- High pressure dry $CO_2$ does not corrode carbon steel pipelines even with the presence of small amounts of methane, nitrogen or other contaminants.
- Cr13 and Super Cr13 show good performance in $CO_2$ environment. However, they are not applicable for temperatures higher than 150°C and in combination with low amounts of $H_2S$ (partial pressure > 1 bar). Cr13 is also sensitive to oxygen corrosion. There is evidence that Cr13 alloy may be susceptible to pitting corrosion by salt water containing combinations of $H_2S$, $CO_2$ and $O_2$ at temperatures as low as $43^{o}C$ ($110^{o}F$). Severe corrosion in Cr13 tubing is also documented in K12-B pilot CCS site, even though conditions were within specifications.
- Austenitic chrome-nickel alloys are susceptible to stress cracking due to both chlorides and sulphides. Their use is not recommended downhole.
- Duplex or superduplex steel (Cr22 and Cr25) is better suited at high temperature and $H_2S$ content, but it can suffer severe corrosion during acid stimulation. It is therefore very important that when using this type of material not to acid wash the well. Duplex and superduplex steel is used in the Sleipner $CO_2$ storage project as casing and tubing, respectively.
- Superaustenitic nickel alloys can also be considered if duplex steel cannot be used. These alloys are significantly more expensive than other available material, and will only be used if it is required.
- Another option could be to use a lower grade steel with an internal coating. However, the coating is not reliable and any breach will lead to rapid corrosion and deterioration of the steel and fragments of the coating may block the perforations.
- Distinction should be made between tubing and casing. Under the condition that tubing-casing annulus will be monitored permanently for pressure build up and $CO_2$ leakage, the casing can be carbon steel. Other considerations are accessibility and remoteness of the well and other factors which may dictate a more robust design. If intervention is

difficult due to location (offshore or populated areas) corrosion resistant material should be selected.
- The part of the casing below the production packer will very likely be exposed to significant corrosion even during the injection phase of the CCS project.
- Metals are prone to corrode when in contact with $CO_2$ also when the well is abandoned due to presence of connate water.

# 6 Corrosion Monitoring

To ensure the project continues in a safe and efficient manner, corrosion should be monitored throughout the project. It is unlikely that $CO_2$ corrosion will not occur at all, and the aim is to closely monitor corrosion, and keep it at an acceptable rate. Corrosion rates are commonly reported in mils per year (mpy) or millimetres per year (mm/yr) of penetration or metal loss, where a mil is equal to a thousandth of an inch(USEPA, 2013). Maximum allowable corrosion rates vary from project to project or even geographically. Target corrosion rates of one mpy (approximately 0.025mm/year) or less are common in wells used in the oil industry. On the other hand, Norsok suggests using a limit of 0.10 mm/year. These acceptable rates cannot be achieved with carbon steel tubulars, unless the environment is dry. From experiments with carbon steel, corrosion rates higher than 10 mm/yr have been observed in a wet $CO_2$ environment (no $H_2S$ present). Laboratory tests from Valourec indicate that the target corrosion rate might not even be achievable for Cr13 casing, as rates higher than 1 mm/yr have been reported under certain conditions(Nagelhout et al., 2009).

The corrosion rate limit refers to general corrosion of the metal, which is the uniform (or near-uniform) thinning of the metal surface. It is important to mention that a low corrosion rate may not be acceptable if localized corrosion (such as pitting) is occurring, whereas a higher rate with a general area type of metal loss may be, in certain cases, a relatively insignificant problem(USEPA, 2013). Inspection of the coupon's surface can yield information about the nature of the corrosion that is taking place (e.g., localized or general attack, presence of pitting or cracking

Corrosion monitoring tools currently used in the industry can be divided into three categories. These are corrosion coupons, corrosion loops and casing inspection logs. Corrosion coupons and loops are simple tools that are also widely used in other industries.

## 6.1 Corrosion coupons

The most common of all corrosion rate measurement tests involves exposing pieces of metal, similar to those in the injection system, to the conditions to which the well materials will be exposed. Small, pre-weighed and measured coupons made of the construction materials are exposed to well fluids for a defined period of time, then removed, cleaned, and weighed to determine the corrosion rate(Allen and Roberts, 1978). Coupons are very simple to use and analyse, and they give a direct measurement of material lost to corrosion.

A coupon is a small, carefully manufactured piece of metal (such as a strip or ring) placed in an appropriate location in the injection well to measure corrosion (Figure 6-1). Coupons are usually placed in the well using wireline equipment. A coupon is made from the same material (or as close as possible) as the well's casing or tubing. It is weighed, subjected to the well environment for a period of time, and then removed and weighed again. The average corrosion rate in the well can be calculated from the weight loss of the coupon(Jaske et al., 1995).

| | Doc.nr: | CATO2-WP3.04-D16 |
| --- | --- | --- |
| | Version: | 2013.12.19 |
| | Classification: | Public |
| | Page: | 19 of 42 |

**Corrosion monitoring**



**Figure 6-1.** Example of corrosion coupons**("Rohrback Cosasco Systems," n.d.)**

Coupons can predict the following types of corrosion when correctly emplaced to ensure appropriate exposure: general corrosion, crevice corrosion, pitting, stress corrosion cracking, embrittlement, galvanic corrosion, and metallurgical structure-related corrosion. However, coupons have several limitations(USEPA, 1987). An extended period of time is required to produce useful data, and coupons can only be used to determine average corrosion rates. Furthermore, corrosion coupons can only measure corrosion in the part of the well in which they are placed.

The differences in the size and thermo-mechanical history of coupons compared with the actual well materials mean that the corrosion rate measured on a coupon cannot exactly match the corrosion rate experienced by the well(USEPA, 1987). Therefore, a lack of serious corrosion in coupons does not necessarily rule out corrosion of well materials.

## 6.2 Corrosion loops

Another method of assessing corrosion is the use of a corrosion loop. A corrosion loop is a section of tubing that is valved so that some of the injection stream is passed through a small pipe running parallel to the injection pipe at the surface of the well. Because the composition of this pipe is the same as the well tubing, it acts as a small-scale version of the well; the only differences are that the loop pipe has a smaller diameter and its temperature (due to its shallower depth) is generally lower(USEPA, 1987).

When the valves are open, some of the injection stream passes through the loop. When the valves are closed, the corrosion loop can be removed from the system and analysed for corrosion. Corrosion rates can be calculated in a similar fashion to the corrosion coupon method. If corrosion is observed in the loop, corrosion is likely occurring in the well tubing. Because the dimensions and temperature of the loop are different from that of the well, the loop may be subject to more or less corrosion than the well itself. In addition, loops cannot measure the corrosion experienced by specific features of the well (such as joints) that may have corrosion-enhancing properties. Due to its shallow placement, corrosion loops are unlikely to provide decent quality data in cases where the injected $CO_2$ is in dry supercritical state.

## 6.3 Casing inspection logs

Casing inspection logs are in situ recordings of casing thickness and integrity, which are carried out by lowering various tools downhole. The purpose of casing inspection logs is to determine the presence or absence of corrosion in the long-string casing/tubing. These logs measure casing thickness or borehole radius. Several different measurement techniques (based on different principles) exist for casing inspection logs. These include physical measurement with a caliper,

| | | |
|---|---|---|
| | Doc.nr: | CATO2-WP3.04-D16 |
| | Version: | 2013.12.19 |
| | Classification: | Public |
| | Page: | 20 of 42 |

**Corrosion monitoring**

electromagnetic phase shift in the magnetic field passing through the tubing or casing, electromagnetic flux leakage due to variations in the tubing or casing, and ultrasonic images of reflected sound waves(USEPA, 2013).

All casing inspection logging tools are wireline based and identify and measure variances, referred to as defects, in the thickness of the casing wall and pipe diameter. Examples of defects are scales, pits or ruts (formed by corrosion, substandard welds at casing couplings, wear from centralizers or collar locators, etc.) and splits that open gaps in the casing. In theory, all of these logs can be performed during injection depending on the injection parameters and the amount of drag forces acting on the equipment under such conditions.

### 6.3.1 Caliper Logs

Caliper logs, also known as multifinger calipers, measure the internal radius of the casing in several directions by using multifinger feeler arms of the tool (Figure 6-2). Because of their rapid logging rate and simple working principle, calipers are among the most commonly used wireline tools in the oil and gas industry. They are available for numerous different pipe sizes, and different number of feeler arms.

A loss of thickness of the casing is evident from a caliper log because the internal radius increases in the area of corrosion. The caliper log is generally reported as internal radius, nominal wall penetration, or average remaining thickness, depending on the logging company. Some logs can even show the variation detected by each arm as side by side traces similar to a seismograph(USEPA, 2013).

The main problem of calipers with regards to corrosion monitoring is their sensitivity to *all* the changes in the inner diameter. Material build-up such as scale will affect caliper readings, and will interpret the casing diameter slower than it actually is. Furthermore, these tools will fail to locate any corrosion that may be building up behind scales. Another limitation of caliper logs is that they will not provide any information about the external condition of the pipe, and the data can only be gathered from the innermost pipe; meaning that the tubing needs to be pulled in order to evaluate casing integrity.

### 6.3.2 Electromagnetic Thickness Logs

Electromagnetic thickness logs are one of two available electromagnetic measuring methods for corrosion monitoring. These logs are carried out by electromagnetic induction tools. The tool has a low frequency emitter coil used to create a magnetic field that passes through the tubing or casing and a receiver coil that measures the shift in the returning magnetic field. The receiver coil is set at a distance where it measures magnetic field outside the coil. The phase shift is proportional to the thickness of the metal and the casing's magnetic permeability(USEPA, 2013). In the meantime, electronic caliper consisting of pad sensors mounted on the tool's centralizer arms measures the magnetic permeability of the void between the tool and the inner wall of the pipe, indicating the average inside diameter (Figure 6-3). With measurements of both the inside diameter and the wall thickness, pipe integrity is evaluated both internally and externally(Acuña et al., 2010).

**Figure 6-2.** An example of a multifinger caliper tool. This particular tool is also capable of temperature measurement. Localised temperature anomalies are an indication of casing leaks, and temperature measurements are used for leak detection regularly (Weatherford, 2010a).

A great advantage of magnetic induction tools over other monitoring tools is that currently two commercially available EM induction tools (namely Schlumberger's EM Pipe Scanner and Baker Hughes' Digital Magnelog) do not require the tubing to be pulled in order to evaluate the condition of the casing. However, the resulting interpretation would be qualitative if more than one string is to be scanned simultaneously. To get quantitative measurements of the casing, a separate run for the tubing is required so that the tubing data could be subtracted from the overall data. Another limitation of electromagnetic induction measurements is that these tools can only detect large sized holes (more than 1 inch diameter).

### 6.3.3   Magnetic Flux Logs

Magnetic flux logs make use of magnetic flux leakage (MFL) technology to determine the location, extent and severity of corrosion and other metal loss defects in tubulars. Flux leakage tools employ a permanent magnet circuit (or and electromagnet) designed to induce high levels of magnetic flux within the pipe wall. Near locations of defects such as corrosion or pitting, some of the flux leaks out of the pipe, and these leaks are detected by the tools sensor arrays(Nielsen and Aller, 1984).

In conventional flux leakage tools, pad-mounted electric coils are used as sensors. Each pad contains upper and lower coils used to measure flux leakage and eddy current, and an eddy coil to produce eddy currents along the inner pipe wall. The coils collect data in the form of induced currents that are converted to casing variations on the log. The pads are set around the tool to give circumferential coverage for the survey. In more recent tools, these electric coils have been replaced by Hall Effect sensors.

| | Doc.nr: | CATO2-WP3.04-D16 |
| --- | --- | --- |
| | Version: | 2013.12.19 |
| | Classification: | Public |
| | Page: | 22 of 42 |

**Corrosion monitoring**

**Figure 6-3.** Centralizer arm with sensor pads of an electromagnetic induction tool (Schlumberger, 2009).

A flux leakage tool can sense defects on the inside or outside of the casing, but since the magnet must be as close as possible to the pipe, a casing examination requires operators to pull the tubing out of the hole. In addition, flux leakage tools are good at measuring sudden thickness changes, but they are not effective if the corrosion is constant or varies slowly over a whole section of pipe.



**Figure 6-4.** Example of a magnetic flux leakage tool(Weatherford, 2010b).

### 6.3.4   Ultrasonic Corrosion Logs

Ultrasonic corrosion logs employ a very high transducer frequency to measure anomalies in the tubing or casing. The emitter/detector is placed at the end of the wireline tool, with centralizers located above. The emitter sends out sound waves and the detector measures the reflected response. The survey can measure anomalies as small as 0.3 inches and measures anomalies both on the inner and outer surfaces of the tubing or casing(Zhang and Akemu, 2010). As the rotating head with the emitter/detector rotates, the electronics keep track of a reference point, and an accurate circumferential image of the pipe is produced.
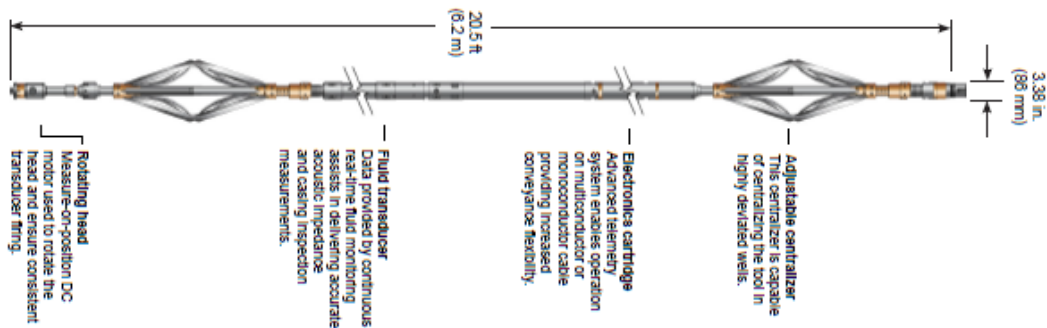
**Figure 6-5**. An image of an ultrasonic casing imaging tool. This tool uses two sets of transducers. The primary emitter/detector is located on the rotating head similar to conventional tools. Meanwhile, a fluid transducer behind continuously monitors the acoustic velocity and impedance of the wellbore fluid (Weatherford, 2010c).

The ultrasonic imaging survey produces images of the surfaces and a log of the thickness. Knowledge of the casing properties is needed to properly interpret the logs. The information used in interpreting the log consist of dimensions, weights and alloys, locations of couplings, locations of wall scratches or other abrasions, locations of perforations, and locations of centralizers.
As the tool relies on the transmission of acoustic waves, ultrasonic corrosion logs (or any other form of acoustic or ultrasonic logs) cannot be run in a gas filled well. A liquid medium will be required if ultrasonic logs are desired in a $CO_2$ injection well. However, since this would induce (or enhance) corrosion, ultrasonic logging tools are highly unlikely to be used as corrosion monitoring tools in CCS projects.

### 6.3.5 Electrochemical sensors

Electrochemical sensors can be used to monitor the corrosion of tubing and casing steel in downhole. ENM and LPR Electrochemical noise measurements (ENM) and linear polarization resistance (LPR) have been used in downhole wireline corrosion monitoring at oil wells (except gas wells) by Saudi Aramco. The system operates at high temperatures (> 150°C). Downhole corrosion monitoring system (DCMS) has been used to inspect different wells in Prudhoe Bay in North America (ref)..

# 7    Electrochemical sensor design

A corrosion rate of a metal in an electrolyte can be obtained by electrochemical measurements such as linear polarization measurements, electrochemical impedance spectroscopy (EIS) and electrochemical noise spectroscopy etc. Assuming that both anodic and cathodic processes are in the linear Tafel region at the corrosion potential, the corrosion current density of a metal can be obtained from polarization curves by Tafel extrapolation method (see Figure 7-2) (Stern and Geary, 1957). If the Tafel slopes on the anodic and cathodic polarization curves for the studied system are known, the corrosion current density can be calculated using the following equation (Fontana, 1986),

$$i_{corr} = b_a \times b_c / (2.3 R_p (b_a + b_c)) = k/R_p \qquad (1)$$

where $b_a$ and $b_c$ are anodic and cathodic slopes, respectively, on the curve; $R_p$ is the polarization resistance and k is the proportional constant. The corrosion rate can be calculated by

$$CR = m/(A \cdot t \cdot \rho) = (i_{corr} \cdot M_w)/(\rho n F) \qquad (2)$$

where m is the mass loss of the metal, A the metal surface area, t the time; $\rho$ the density of the metal, $M_w$ the molecular weight of the metal, n the number of electrons exchanged in the electrochemical reaction and F the faraday's constant.

To do LPR and EIS measurements, three electrodes, named as working electrode (WE), reference electrode (RE) and counter electrode (CE), are normally used (see figure 7-1a). For ENM two identical working electrodes and a reference electrode are used (see figure 7-1b) (Homborg et al., 2013, 2012). For corrosion monitoring, the electrodes can be made using the same materials as those to be monitored.
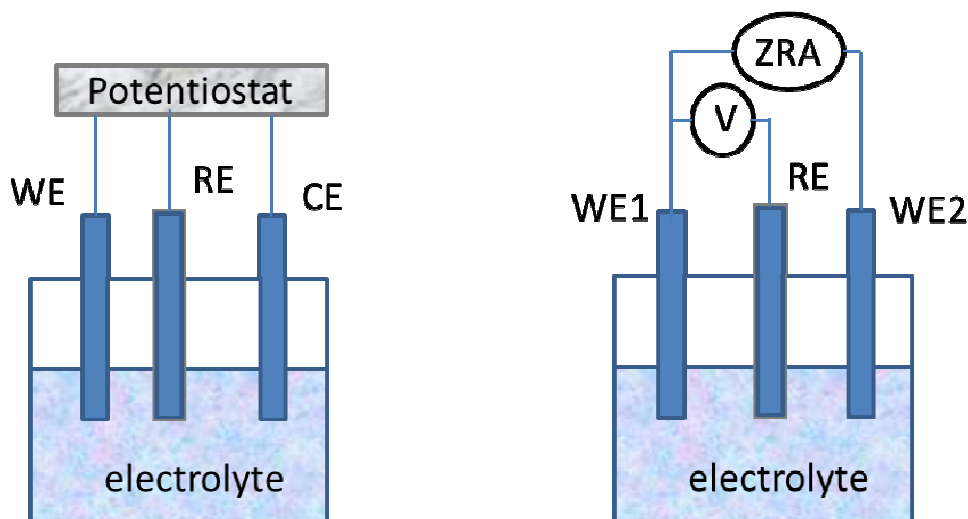


**Figure 7-1.** illustration of the electrochemical cells for LPR and EIS (a), and for ENM (b) measurements.

![cato2 logo]

| | |
|---|---|
| Doc.nr: | CATO2-WP3.04-D16 |
| Version: | 2013.12.19 |
| Classification: | Public |
| Page: | 25 of 42 |

**Corrosion monitoring**

## 7.1    Corrosion of steels in brine + CO₂

The corrosion of casing steel API N80 in $CO_2$-saturated brine has been studied experimentally, using formation water composition typical for North Sea reservoirs. The aim of this study is to investigate the corrosion behaviour of the casing steel under realistic $CO_2$ storage conditions. This knowledge will help corrosion monitoring methodologies of the casing steel (Arts and Winthaegen, 2005).

### 7.1.1    Materials

The samples were cut from N80 steel tubes. The nominal composition of the N80 steel is presented in Table 7-1. To make an electrical connection it was necessary to weld a thread to the sample as the working electrode. The samples were embedded in epoxy coating and left one surface to be exposed to the electrolyte. After mechanical grinding (until 4000 grid SiC paper), samples were cleaned in ultrasonic ethanol before being transferred to an autoclave. The exposure area is about 2.8 cm$^2$.

Table 7-1. Nominal composition of the steel (wt. %)

| Element | C | Mn | Si | S | P | Cr | Mo | Ni | Al | Fe |
|---|---|---|---|---|---|---|---|---|---|---|
| N80 | 0.29 | 1.48 | 0.34 | 0.014 | 0.012 | 0.24 | 0.09 | 0.08 | 0.04 | rest |

### 7.1.2    Electrochemical measurements

The brine solution used in the study contained 130 g/l NaCl, 22.2 g/l $CaCl_2$ and 4 g/l $MgCl_2$. The $CO_2$ was charged in the brine in the autoclave at different pressures (60, 80 and 100 bar) and at 45°C. The solution was stirred with a stirrer in a rotation speed of 600/min to make the solution homogeneous.

The electrochemical measurements were performed using three electrode cells, the steel as the working electrode, a KCl saturated Ag/AgCl electrode as the reference electrode and a platinum mesh as the counter electrode. The corrosion properties were studied using open circuit potential (OCP), linear and potentiodynamic polarization measurements. The linear polarization to determine the Rp was performed by scanning the potential from -20 mV vs. OCP to + 20 mV vs. OCP. The potentiodynamic measurements, to determine the Tafel slopes, were performed by scanning the potential from -250 mV vs. OCP to +250 mV vs. OCP. The corrosion current density and the corrosion rate were calculated from the Tafel slopes and the polarization resistance.

### 7.1.3    Mass loss measurements

The steel samples were cleaned and weighed before exposure to the brine and $CO_2$. After immersion for 32 days, the samples were removed from the autoclave, rinsed immediately with running tap water to remove salts. Then the samples were chemically cleaned for 10 min. at 20°C in a fresh solution prepared as follows: mixing 1000 ml of hydrochloric acid (sp gr 1.19) with 1000 ml deionized water and adding 10 g of hexamethylenetetramine. After cleaning, the samples were rinsed in deionized water and dried in flow air. The mass loss was determined by reweighing and subtracting the sample mass after exposure from its original mass.

| | Doc.nr: | CATO2-WP3.04-D16 |
| --- | --- | --- |
| | Version: | 2013.12.19 |
| | Classification: | Public |
| | Page: | 26 of 42 |

**Corrosion monitoring**

### 7.1.4    Surface analysis

After immersion test in the autoclave, the surface of the specimens and corrosion products deposited on the specimens were analysed using SEM and EDS. The components of corrosion products were analysed by XRD using Co kα radiation.

The methods and conditions are summarized in Table 7-2.

Table 7-2. Methods and conditions

| Solution | Brine + $CO_2$ 60, 80, 100 bar; 45 °C | Brine + $CO_2$ 80 bar; 45 °C | Brine + $CO_2$ 100, 130, 150 bar; 80 °C |
| --- | --- | --- | --- |
| Polarization | √ | √ | √ |
| Mass loss test | | √ | |
| SEM, XRD | | √ | |

### 7.1.5    Polarization measurements

Figure 7-2 shows a typical polarization curve for the N80 steel in brine plus $CO_2$ at 80 bar and 45°C after exposure for 2 hours. The anodic and cathodic slopes were determined from the polarization curves. The average k value is 25 mV for this system. Corrosion current density $i_{corr}$ and corrosionrate were calculated from the curves using the equation (1) and (2), respectively.
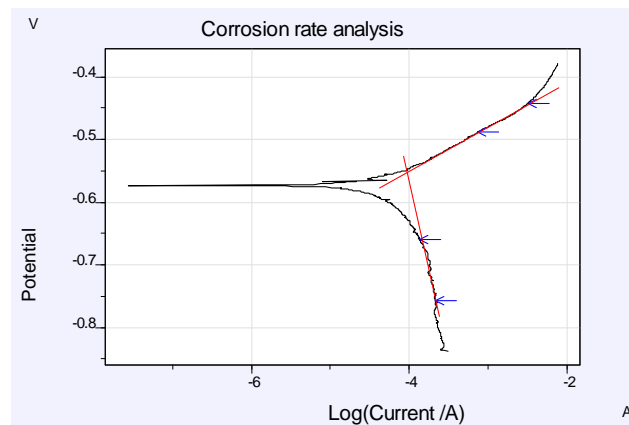


**Figure 7-2.** Polarization curve for the N80 steel in brine plus $CO_2$ at 80 bar and 45°C after exposure for 2 hours.

| | Doc.nr: | CATO2-WP3.04-D16 |
|---|---|---|
| | Version: | 2013.12.19 |
| | Classification: | Public |
| | Page: | 27 of 42 |

**Corrosion monitoring**

Figure 7-3 shows the corrosion rates calculated from the polarization curves. The corrosion rate is as high as 6 mm/y at the beginning and decreases to 0.3 mm/y after one week for N80 steel in the solution at 80 bar and 45°C. The corrosion rate at all three pressures decreases with time. The corrosion rate at 100 bar decreases a little bit slowly that at 60 and 80 bar within 4 days. After 4 days the corrosion rate at 100 bar is lower than at 60 bar, which is in agreement with the reference(Seiersten, 2001).
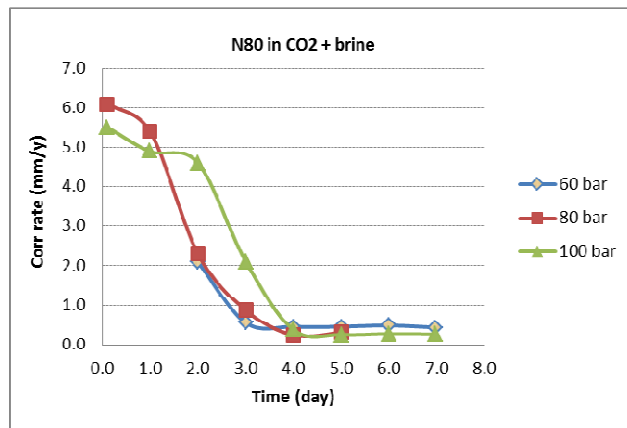


**Figure 7-3.** Corrosion rate as a function of time for N80 steel in the brine plus $CO_2$ at 45°C and different pressure.

Figure 7-4 shows the open circuit potential as a function of time for N80 steel in the brine plus $CO_2$ at 80 bar and 45 °C. The increase of potential with time (from -0.6 $V_{Ag/AgCl}$ at the beginning to -0.18 $V_{Ag/AgCl}$ at day 5 suggests that the surface is active at the beginning and then is polarized or covered with corrosion products. The real surface area of the steel exposed to electrolyte decreased with time and the average corrosion rate was slowing down.
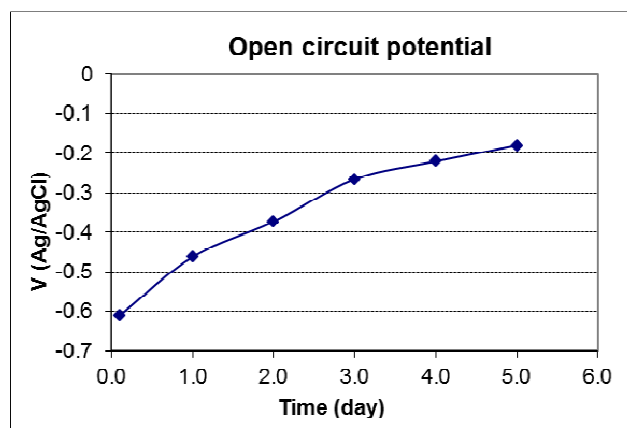


**Figure 7-4.** OCP values as a function of time for N80 steel in the brine plus $CO_2$ at 80 bar and 45°C.

| | Doc.nr: | CATO2-WP3.04-D16 |
|---|---|---|
| | Version: | 2013.12.19 |
| | Classification: | Public |
| | Page: | 28 of 42 |

**Corrosion monitoring**

The linear polarization measurements for N80 steel in brine and $CO_2$ at higher pressures were also performed. Figure 7-5 shows the corrosion rates in different pressures for the N80 steel in brine plus $CO_2$ at 80°C. The corrosion rate increased significantly when the pressure reached 150 bar.
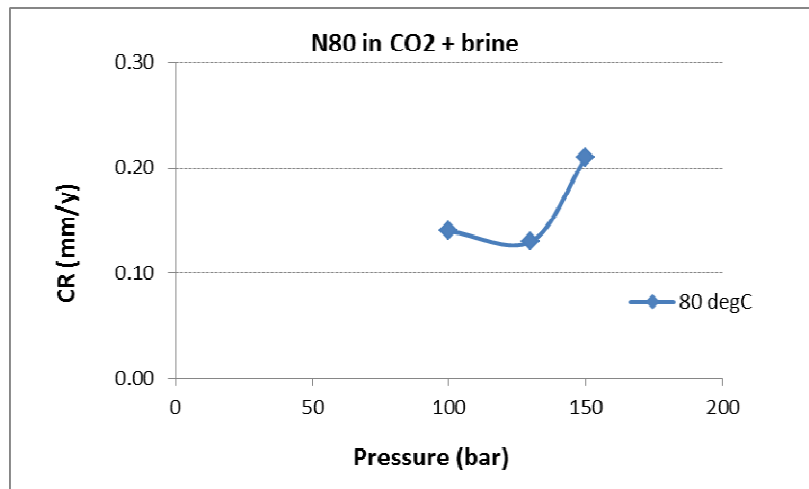


**Figure 7-5.** Corrosion rate for N80 steel in the brine plus $CO_2$ at different pressures and at 80°C, after exposure for 4 hrs.

### 7.1.6    Corrosion rate

The mass loss data are presented in Table 7-3. It shows an average corrosion rate of 0.06 mm/y measured in 32 days, which is lower than that measured by polarization measurements in a stirred solution in a week. But this experiment shows, again, that the average corrosion rate decreases with time.

Table 7-3. Mass loss rate measured for N80 steel exposed to the brine and $CO_2$ at 80 bars and 45°C for 32 days

| Sample | Mass before (g) | Mass after (g) | Mass loss (g) | Surface area (cm$^2$) | Mass loss/area (mg/cm$^2$) | Corrosion rate (mm/y) |
|---|---|---|---|---|---|---|
| 1 | 122.836 | 121.728 | 1.108 | 246.67 | 4.49 | 0.066 |
| 2 | 116.573 | 115.689 | 0.884 | 235.15 | 3.76 | 0.056 |
| 3 | 120.240 | 119.390 | 0.850 | 243.48 | 3.49 | 0.052 |

### 7.1.7    Corrosion morphology

The surfaces of some samples after exposure to $CO_2$ and brine have been analyzed by SEM and EDS. Figure 7-6 shows (a) an SEM image and (b) the EDS spectrum measured in the square area 1 shown in (a) for an N80 sample after exposure to brine plus $CO_2$ at 80 bar and 45°C for 32

| | |
|---|---|
| Doc.nr: | CATO2-WP3.04-D16 |
| Version: | 2013.12.19 |
| Classification: | Public |
| Page: | 29 of 42 |

**Corrosion monitoring**

days. The corrosion products on the sample surface are crystalline, composed of C, O, Fe and Ca. Calcium signal present in the EDS spectrum means that partial calcium cations in the brine has precipitated and combined in the surface film.

Figure 7-7 shows the XRD diagram and the fit phases for N80 steel after exposure to the brine plus $CO_2$ at 80 bar and 45°C for 32 days. The best fit of the patterns is dolomite $CaMg_{0.77}Fe_{0.23}(CO_3)_2$.

The layer formed on the surface of the casing steel in the condition investigated is compact, which hinders the corrosion process of the steel. That is why the corrosion rate decreases with time and is very low after immersion exposure for 32 days in the autoclave.



(a)                                              (b)
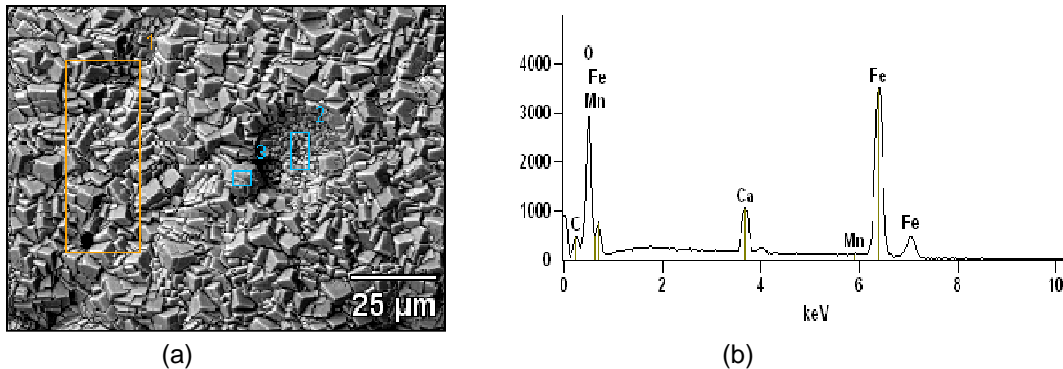
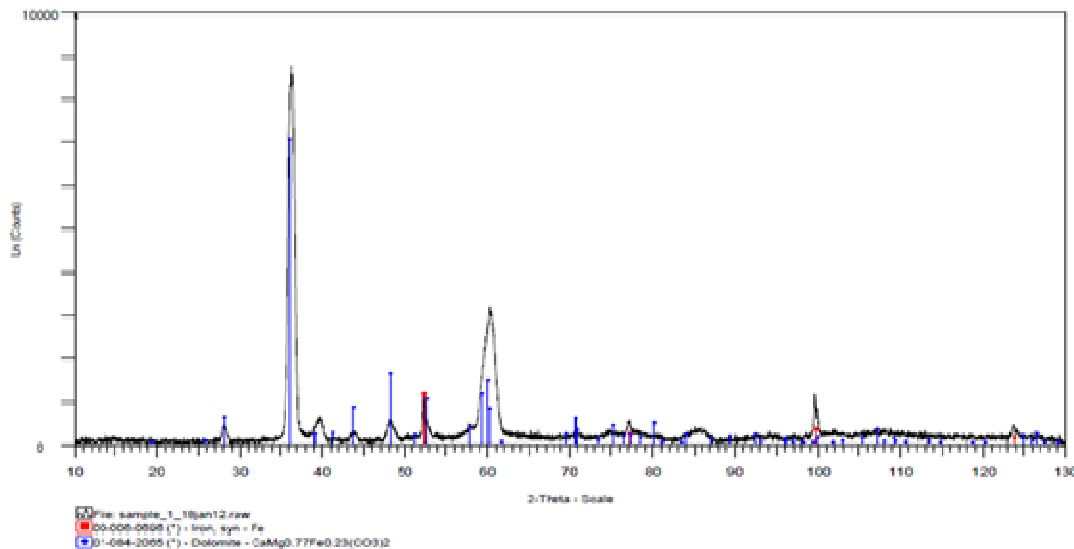**Figure 7-6.** SEM image (a) and EDS spectrum (b) for N80 after exposure to the brine plus $CO_2$ at 80 bar and 45°C for 32 days.



**Figure 7-7.** XRD spectrum and fit phases for N80 after exposure to the brine plus $CO_2$ at 80 bar and 45°C for 32 days.

Doc.nr:         CATO2-WP3.04-D16
Version:       2013.12.19
Classification:  Public
Page:           30 of 42

**Corrosion monitoring**

## 7.2 Corrosion of steels in brine + $CO_2$ + $H_2S$

The nominal compositions of the N80 steel and Cr13 steel are presented in Table 7-4. For electrochemical measurements, the samples were embedded in an epoxy coating and left one surface to be exposed to the electrolyte. After mechanical grinding (until 4000 grid SiC paper), samples were cleaned ultrasonically in ethanol before being transferred to an autoclave. The exposure area is about 2.8 $cm^2$ for the N80 steel, 5 $cm^2$ for the Cr13 steel. For the mass loss test the bare steel samples are used.

Table 7-4: Nominal composition of the steel (wt. %)

| Element | C | Mn | Si | S | P | Cr | Mo | Ni | Al | Fe |
|---------|------|------|------|-------|-------|------|------|------|------|------|
| N80 | 0.29 | 1.48 | 0.34 | 0.014 | 0.012 | 0.24 | 0.09 | 0.08 | 0.04 | rest |
| Cr13 | 0.08 | 1.0 | 0.9 | 0.013 | 0.03 | 13.5 | - | 0.58 | - | rest |

### 7.2.1 Polarization measurements for Cr13 steel

Figure 7-8 shows a typical polarization curve for Cr13 steel in the brine plus $CO_2$ at 130 bar and 80 °C for 16 hours. The corrosion potential is -0.08 $V_{Ag/AgCl}$ and the corrosion current density is $5\times10^{-6}$ $A/cm^2$. The corrosion rate is about 0.06 mm/y. A passivation curve is observed in a potential range of 0.2V and the breakdown potential is 0.17 $V_{Ag/AgCl}$.
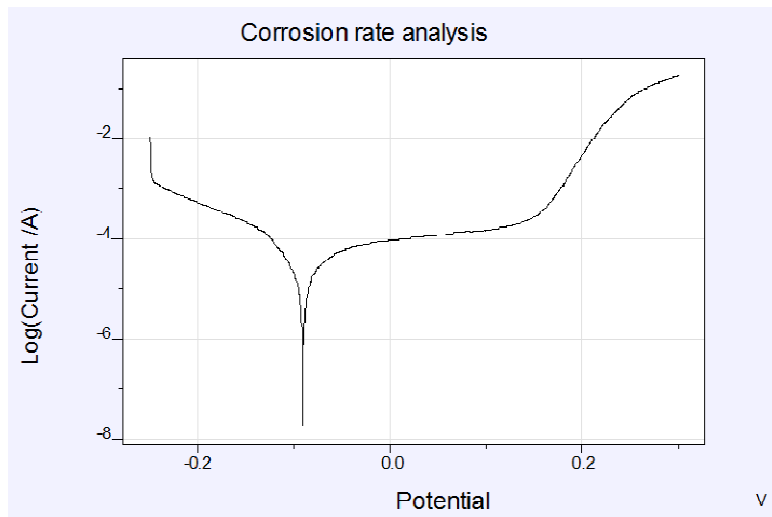


**Figure 7-8.** polarization curve for Cr13 in the brine plus $CO_2$ at 130 bar and 80°C, after exposure for 16 hrs.

### 7.2.2 Corrosion rate

The corrosion rates calculated from mass loss tests in the brine plus $CO_2$ and 1%$H_2S$ solutions at 130 bar and 80 °C are presented in Table 7-5. The N80 steel has a corrosion rate as high as 0.45 mm/y for 36 days. The corrosion layer deposited on the surface was analyzed by XRD. The components in the layer contain mainly FeS and $FeCO_3$ (see figure 7-9).

The Cr13 steel shows a very low average corrosion rate for the immersed samples. The uniform corrosion rate is 1 orders lower than for the N80 steel. The samples exposed to the gas phase do not show much corrosion, but the half-immersed samples showed severe localized corrosion (see figure 7-10). The pit depth was investigated by microscope via cross section view (see figure 7-11). The pit depth is about 55 µm after exposure for 33 days for the half-immersed samples. The pit penetration rate is about 0.6 mm/y for the half-immersed samples, while it is 0.49 mm/y for the fully immersed samples.

Table 7-5: average corrosion rate (mm/y) of steels in brine plus $CO_2$ + 1%$H_2S$ at 130 bar and 80 °C by mass loss test

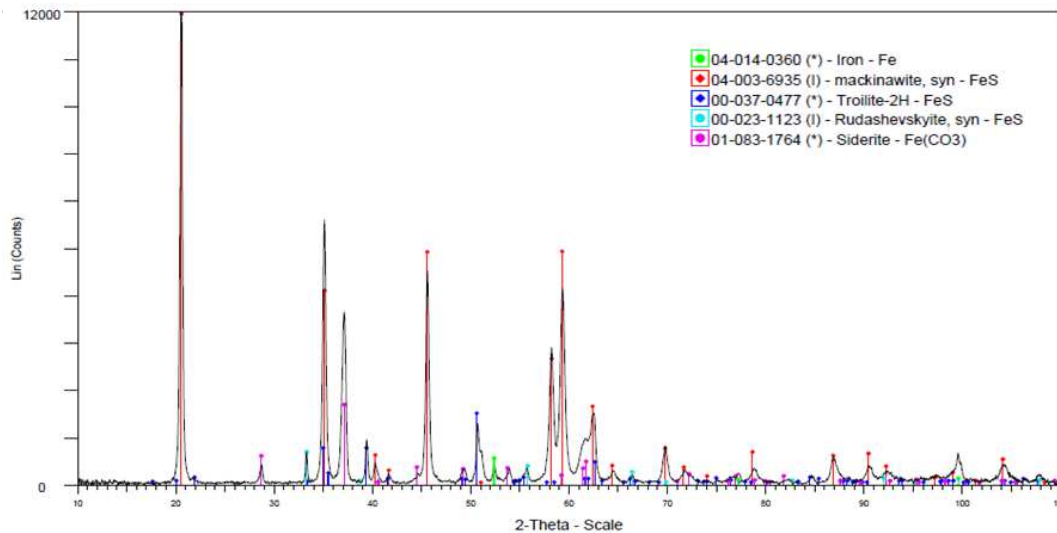| Materials | immersion | half-immersion | in gas phase |
|---|---|---|---|
| N80 | 0.45 | 0.29 | 0.1 |
| Cr13 | 0.015 | 0.019 | 0.0005 |



**Figure 7-9.** XRD diagram for N80 steel in the brine plus $CO_2$ + 1% $H_2S$ at 130 bar and 80°C for 36 days.
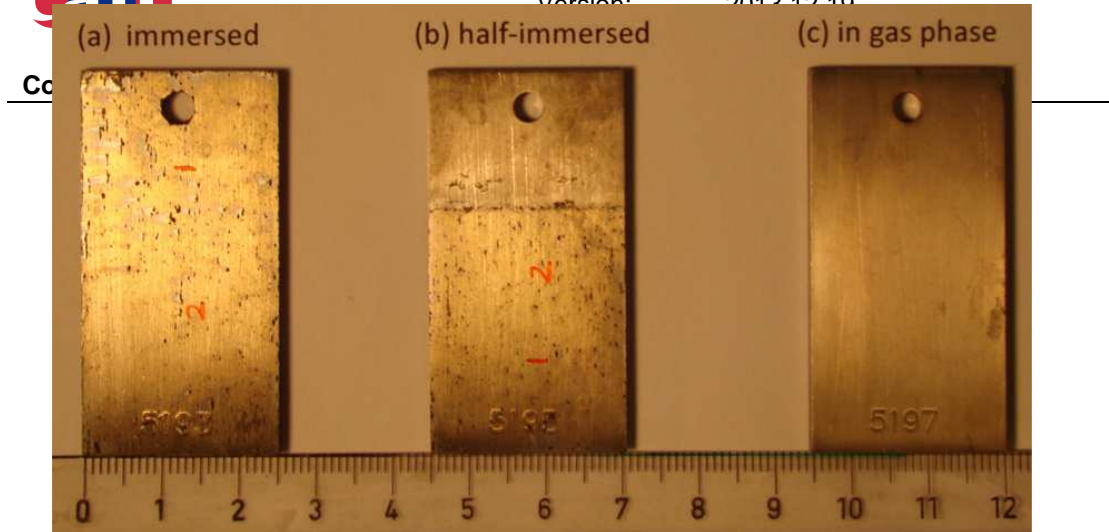
**Figure 7-10.** Cr13 samples exposed to the brine plus $CO_2$ + 1% $H_2S$ at 130 bar and 80°C for 33 days.

Previous work shows that the corrosion rate of the N80 steel is as high as 6 mm/y at the beginning in the brine plus $CO_2$, but it decreases with time due to the formation of a siderite $FeCO_3$ layer on the surface (Zhang et al., 2013). The present work shows that the average corrosion rate is as high as 0.45 mm/y after exposure for 36 days. It indicates that the $H_2S$ has an adverse effect on the corrosion of N80 steel. This adverse effect of $H_2S$ on corrosion of steels has also been reported by El Alami et al.(El Alami et al., 2011).
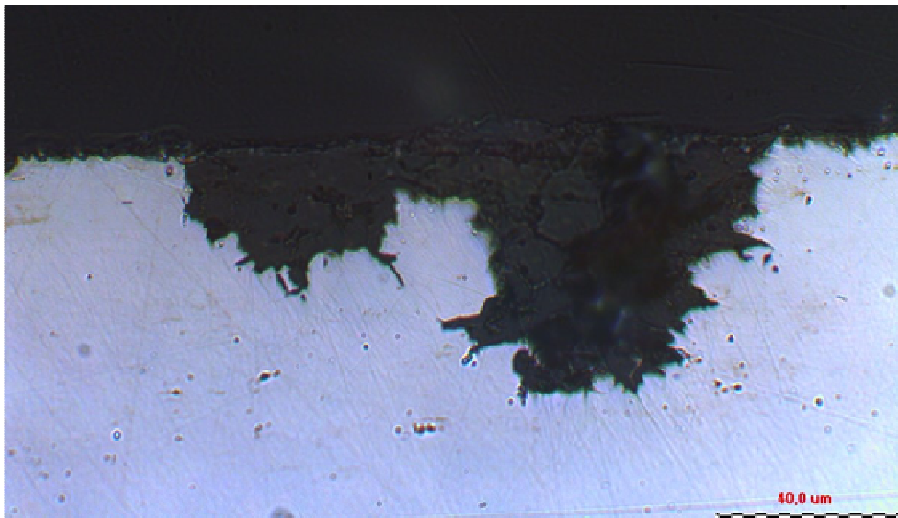


**Figure 7-11.** cross section image for a Cr13 sample exposed to the brine plus $CO_2$ + 1% $H_2S$ at 130 bar and 80°C for 33 days.

The Cr13 steel has a lower uniform corrosion rate than the N80 steel in the brine plus $CO_2$ and 1%$H_2S$ at 130 bar and 80°C. This is attributable to its passivation capability. However it is susceptive to localized corrosion that has to be paid attention to application when using this steel in a $CO_2$/brine.

## 7.3   Probe Design

The corrosion resistance for a metal in a given environment can be measured by electrochemical methods, such as LPR, EIS and ENM measurements. So corrosion probes can be designed to monitor corrosion of steel by measuring LPR, EIS or ENM via the electrochemical cell composed of the same steel. A multi-electrode probe system was designed that used all these three electrochemical techniques to compare their sensitivity and reliability.

The probe system is schematically illustrated in figure 7-12. Electrodes were made of N80 carbon steel, the same steel used as casing. Every electrode was coated with a special coating to avoid crevice corrosion. The titanium rod was oxidized before the measurement. The probes were tested in autoclave to simulate the downhole conditions. As shown in Figure 7-12, two of carbon steel electrodes were used as working electrodes (WE) for LPR and EIS measurements separately. The other 3 electrodes were as WE1, WE2 and RE for ENM measurement.

As a comparison, a separated Ag/AgCl reference electrode was set in the autoclave too. A platinum counter electrode for EIS and LPR measurements were also tested..
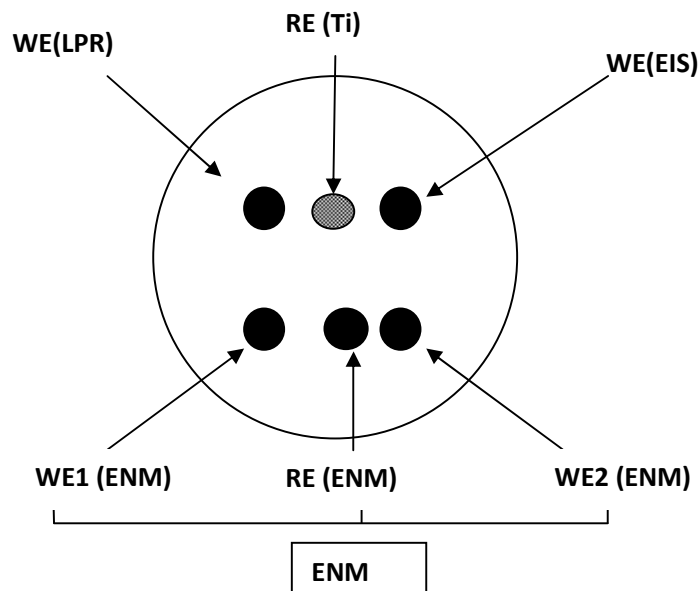


**Figure 7-12.** Schematic structure of multi-electrode probe

The probe was studied using three  electrochemical methods as described above for monitoring corrosion process in $CO_2$ plus brine environment. All measurements were carried out in an autoclave containing a volume of 0.8 litre brine. The brine contains 130g/l NaCl, 22.2g/l $CaCl_2$ and 4 g/l $MgCl_2$. $CO_2$ was charged into the autoclave to reach the target pressure. The pressure was set at about 100 bar, and the temperature was 60°C. All cables were magnetic shielded to avoid noise or other influence from the outside.

### 7.3.1   Environmental effect on results

The magnetic electrical shield is necessary to electrochemical measurements, especially for ENM. The ENM is very sensitive to the foreign disturbance.
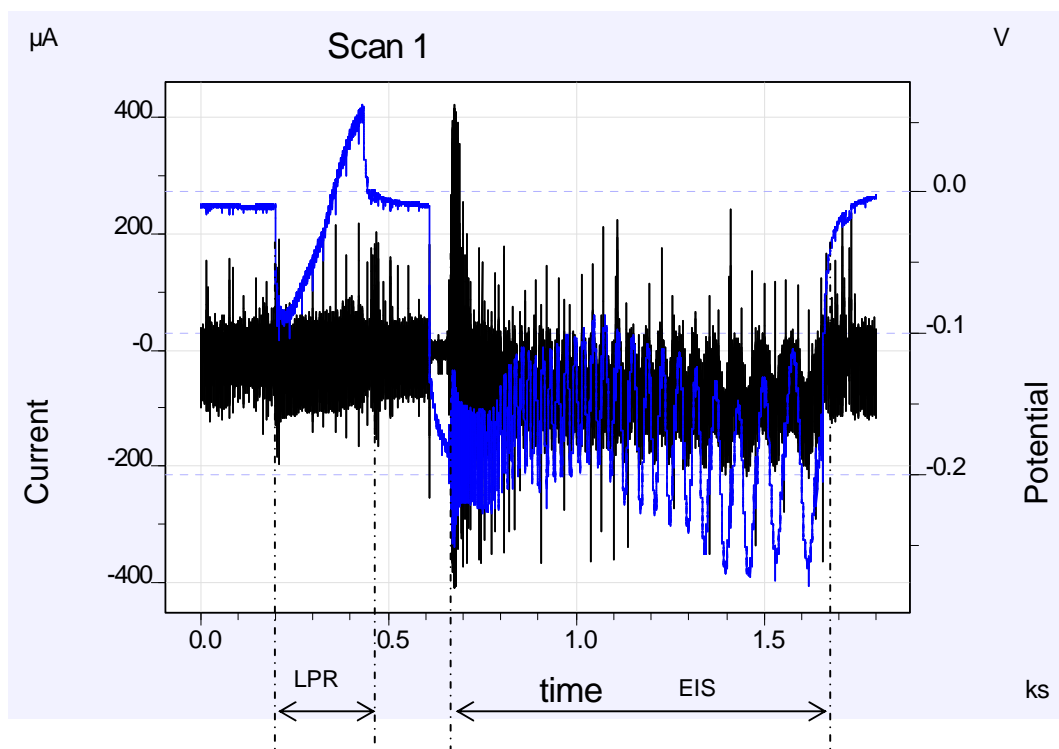
**Figure 7-13.** Running ENM measurements when LPR or EIS measurements were running. The blue line is for potential and the black line is for current.

The EIS, LPR and ENM measurements cannot be done at the same time. As shown in Figure 7-13, both the potential noise and the current noise were changed dramatically when EIS/LPR was performing at the same time.

### 7.3.2 Comparison of corrosion resistance obtained by EIS, LPR and ENM with $CO_2$

The probes were tested in brine plus $CO_2$ in an autoclave at 100bar and 60°C. Figure 7-14 shows the Bode impedance plots for a probe measured as a function of time. The resistance at the high frequency side reflects mainly the Ohmic resistance of the electrolyte. The resistance at the low frequency side reflects the polarization resistance which is related to the corrosion resistance of the materials in this electrolyte. The results show that the resistance decreases within 24 hours and then increases after 32 hours. The phase angle (Theta) shows two peaks which means two time constants (RC,) in an equivalent circuits needed to fit the curves. One time constant is for the surface layer (capacitive behaviour) and the other one is for the electrical double layer (interfacial).

The resistances measured by LPR, EIS and ENM as a function of time are shown in Figure 7-15. The three types of measurements give different resistance values, but they show the same trend. The corrosion resistance was lower than 100 ohms, but after immersion for 100 h, the corrosion resistance increased and stayed between 150 and 450 ohms.
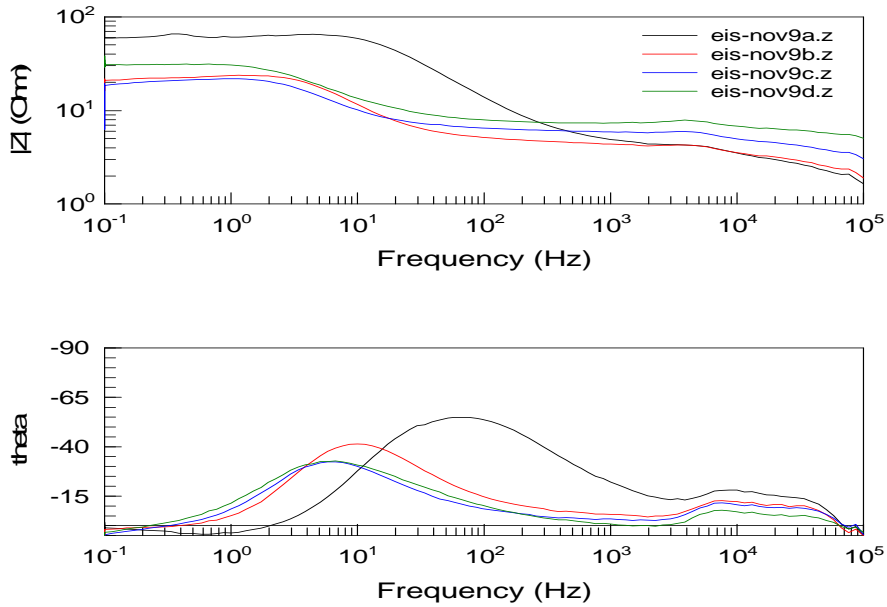
| | Doc.nr: | CATO2-WP3.04-D16 |
| --- | --- | --- |
| | Version: | 2013.12.19 |
| | Classification: | Public |
| | Page: | 35 of 42 |

**Corrosion monitoring**

**Figure 7-14.** impedance plots for N80 probe after immersion for 1 h (eis-nov 9a), 13 h (eis-nov 9b), 24 h (eis nov 9c), and 35 h (eis nov 9d).
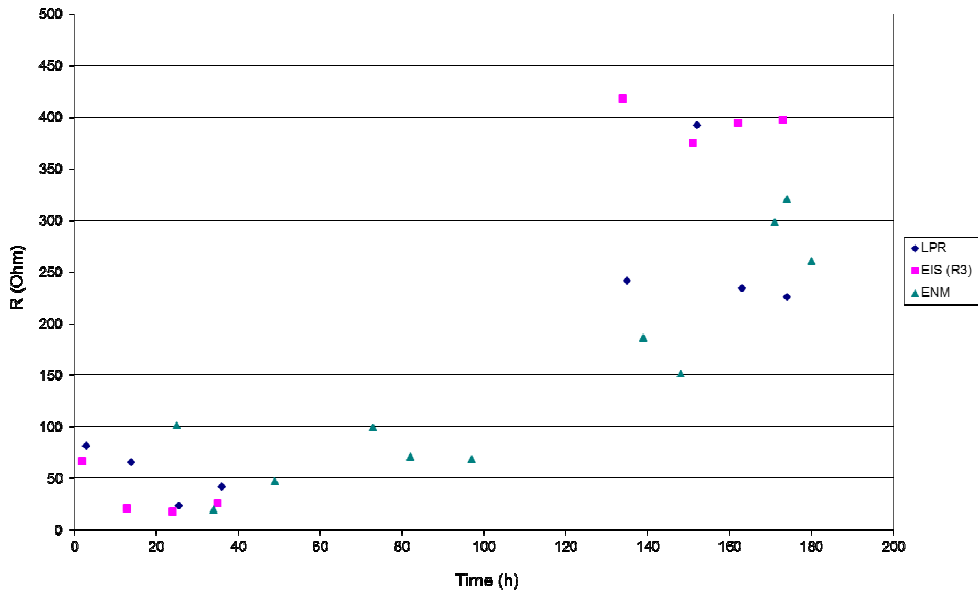


**Figure 7-15.** The corrosion resistance of probe 3 measured by LPR, EIS and ENM measurements in brine plus $CO_2$ at 100bar and 60°C.

### 7.3.3 Pressure variation effect

The pressure changes when $CO_2$ is injected or released. How does the pressure variation affect the electrochemical measurements? Figure 7-16 shows the corrosion resistance measured by EIS, LPR and ENM under the same condition as in section 7.3.2, but with $CO_2$ re-filling. As described in section 7.3.2, the corrosion resistance increased to more than 150 Ohm after 100 hrs. However, the corrosion resistance decreased to less than 100 Ohm after re-charging $CO_2$, and it kept at a low value even after 500 hours immersion.
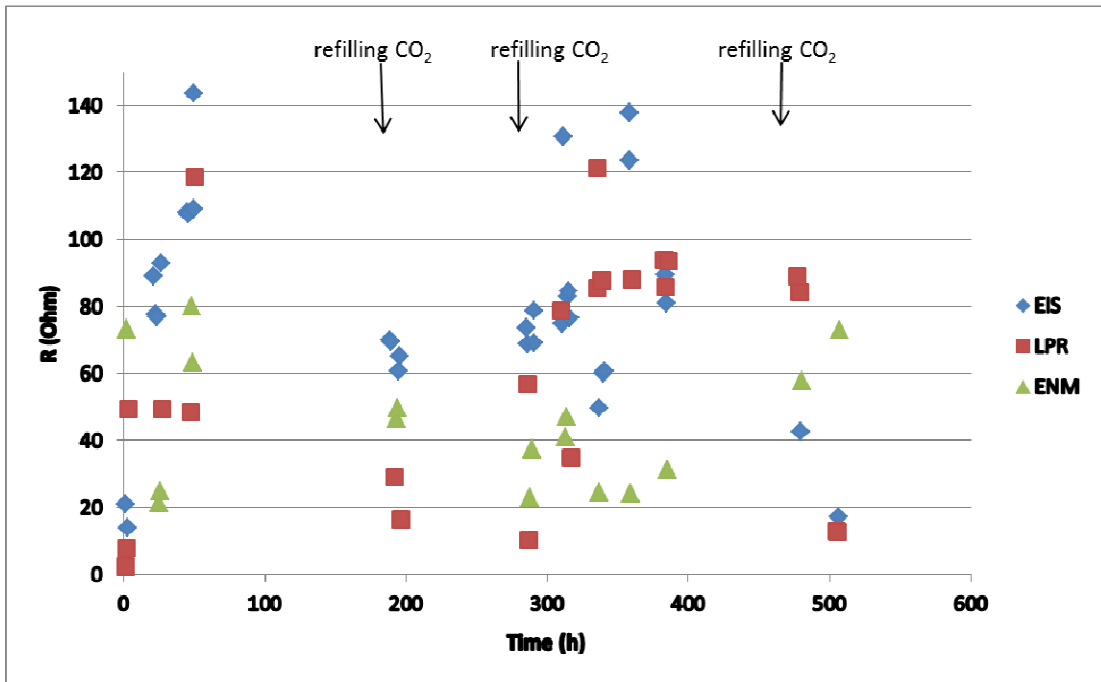


**Figure 7-16.** Corrosion resistance by EIS, LPR and ENM measurements with $CO_2$ re-filling/charging.

In order to investigate the pressure variation effect on the corrosion resistance, which may happen in a well, EIS, LPR and ENM were carried out under different pressures by releasing $CO_2$. First $CO_2$ was charged into the autoclave to increase the pressure and the corrosion resistance was measured. Then $CO_2$ was released to reduce pressure and the corrosion resistance was measured again. Two cycles were performed and the results are shown in Figure 7-17. The corrosion resistance was measured by EIS and LPR, respectively. The corrosion resistance increased when the pressure decreased. Their relationship is linear in both cases:

$$Rc = 18.82 \ P + 2972 \quad r^2 = 0.814 \qquad (3)$$

$$Rc = 28.46 \ P + 3994 \quad r^2 = 0.615 \qquad (4)$$

Equation (3) is for LPR and equation (4) is for EIS, where r is the correlation coefficient. However, the corrosion resistance measured by ENM was scattered. This is because the ENM is sensitive to environments. Section 7.3.2 has shown that it takes more than 100 hrs for the system to reach a stable status, One or two hours during pressure variation was too short for system to reach a stable phase.
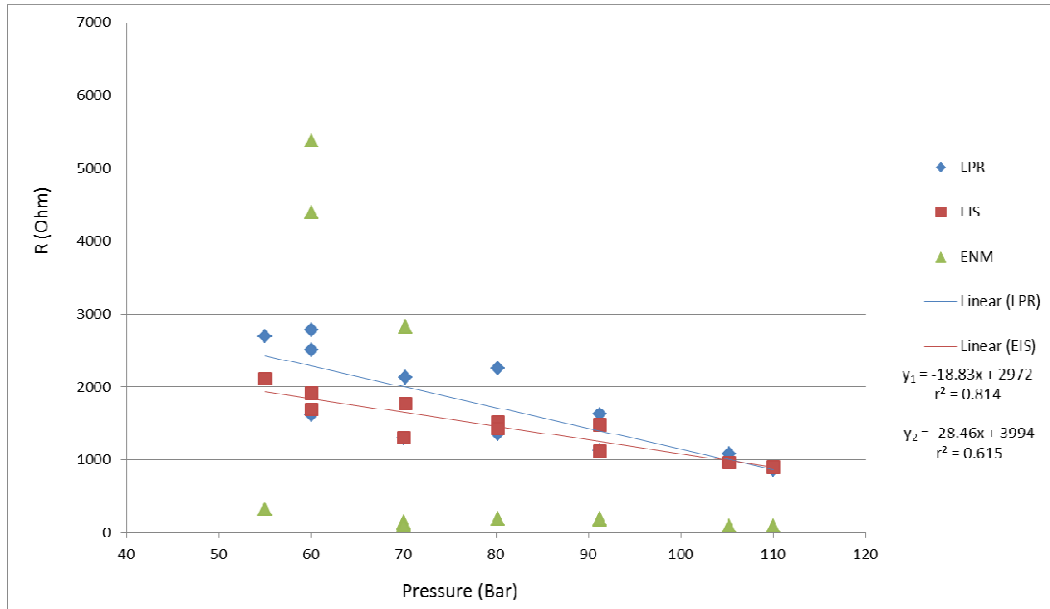
**Figure 7-17.** Corrosion resistance measured using EIS, LPR and ENM as a function of pressure.

### 7.3.4    Influence of electrochemical measurements on the probe morphology

Figure 7-18 shows the images of the CS probe after immersion and measurements for over 500 hrs. The surface image of each electrode was shown as well. It shows that the electrodes used for EIS  and LPR measurements were much different from the electrodes for ENM. The later was almost not influenced by measurements. The electrodes for EIS and LPR measurements were corroded. However, the electrodes for ENM (WE1 and WE2) were similar to the reference electrode for ENM (e). This indicates that the EIS and LPR measurements have changed the probe surface morphology after several measurements, because an applied potential (±10 mV). The ENM did not change the sample surface morphology. As a passive detector ENM needs not apply potential as LPR and EIS need, which has less affection on the probe after long working time.
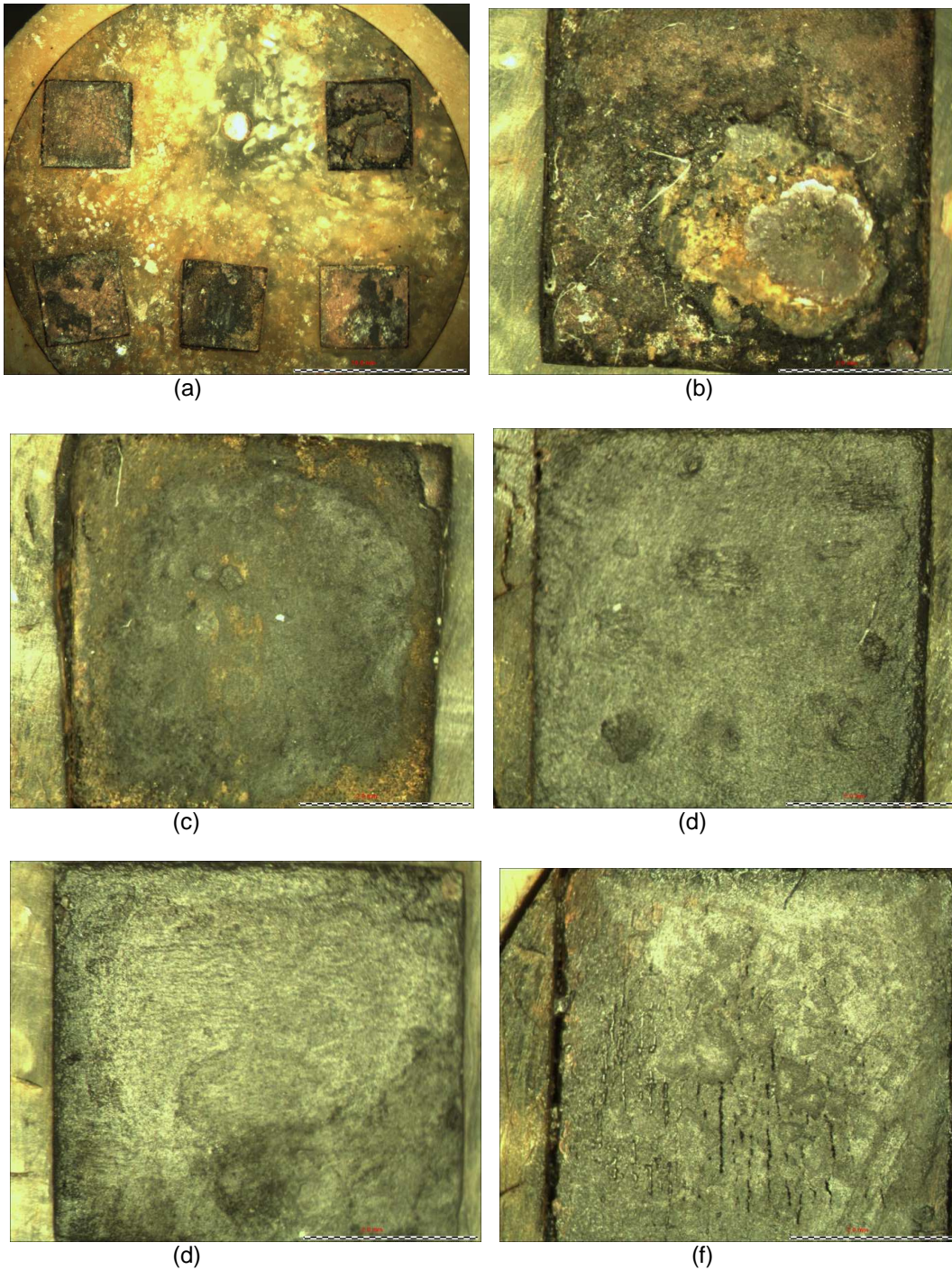
(a)

(b)

(c)

(d)

(d)

(f)

**Figure 7-18**. Surface images of CS probe after 500 hrs immersion (a), and electrodes for EIS (b), LPR (c), ENM WE1 (d), ENM WE2 (e), and ENM reference (f).

| | |
|---|---|
| Doc.nr: | CATO2-WP3.04-D16 |
| Version: | 2013.12.19 |
| Classification: | Public |
| Page: | 39 of 42 |

**Corrosion monitoring**

### 7.3.5    Stainless steel probe

Downhole with higher pressure and temperature, the carbon steel may not have high enough corrosion resistance to withstand the corrosive environment. Stainless steels or corrosion resistive alloys (CRA) can be used. The corrosion study in section 7-2 has shown that the general corrosion rate of Cr13 steel in $CO_2$ is very low, but it suffers localized corrosion.

Normally the corrosion rate measured by LPR and mass loss measurements cannot reflect the localized corrosion rate. Although it is difficult to predict the localized corrosion rate, ENM can be used to distinguish if it is localized corrosion or general corrosion and EIS can be used to study the capacitive behavior of the passive layer on the surface. This needs further investigation.

## 7.4    Sensitivity of the corrosion probe

Three electrochemical techniques are applied for corrosion monitoring test: EIS, LPR and ENM. All techniques have shown similar corrosion resistance level for N80 steel in $CO_2$. The system reached a relatively stable phase after about 100 hours, where the corrosion resistance rises from about 50 Ohm at the beginning to above 150 Ohms. Once the system has reached a stable phase, the corrosion resistance is in a high level. The corrosion resistance keeps at a low level, lower than 100 Ohm when $CO_2$ is injected into the system. The corrosion resistance increases when $CO_2$ is released. A linear relationship is observed.

All these three techniques can be applied to measure the corrosion resistance of the material in the down well, however, each technique has its strong and weak points, that are shown in the Table 7-7. Based on their characteristics, the ENM is a good option for online monitoring because of its good integration, long life time. However, this technique is sensitive to all electromagnetic disturbances. The set-up must be magnetically shielded. Both EIS and LPR have influence on the probe surface when repeating the measurements, though the applied potential is small (±10 mV vs OCP). Therefore the measuring time for these techniques should be limited; the method is not good for a long period repeat. However, both techniques are good options for routine inspection, such as a once-per-year- check of the corrosion resistance/rate of the tubes. They are less affected by environments, and data analysis is comparatively easy. Furthermore, they can be used as calibration tools for ENM.

Table 7-7: The characteristics of LPR, EIS, and ENM on corrosion monitoring

| | LPR | EIS | ENM |
|---|---|---|---|
| Environments influence | No | Yes | Yes |
| Reference Electrode essential | Yes | Yes | No |
| Sample surface change | Yes | Yes | No |
| Easy data analysis | Yes | Yes | No |
| Result reproducible | Yes | Yes | No |
| Online data record | Yes | YES | Yes |
| Long term monitoring | No | No | Yes |

# 8 Conclusions

Corrosion of steels downhole, materials selection and corrosion monitoring tools have been surveyed. The corrosion of API N80 and Cr13 steels have been investigated. Cr13 steel Corrosion sensors made of N80 steel based on electrochemical measurements have been designed and tested in brine plus $CO_2$ in autoclave in simulating the practical downhole conditions.

The corrosion rate decreases with time due to formation of a dolomite layer $CaMg_{0.77}Fe_{0.23}(CO_3)_2$ on steel surface. The corrosion rate increases significantly when pressure reaches 150 bar at 80°C (Section 7-1).

The Cr13 steel has a lower general corrosion rate than N80 steel, but it suffers pitting corrosion. In $CO_2$ plus $1\%H_2S$ the localized corrosion rate for Cr13 is as high as 0.6 mm/y (Section 7-2).

The corrosion sensors are sensitive to the environmental electromagnetic disturbance and the probe systems have to be well shielded from these disturbance.

The corrosion sensors can measure corrosion resistance (and corrosion rate) of casing steel N80 downhole using LPR, EIS and ENM techniques. All three modes can reflect the corrosion level of the casing steel though they give different values. The LPR and EIS modes can also reflect the pressure change. The ENM mode is more sensitive to the environmental disturbance. The ENM is suitable for long term monitoring and the other two modes are suitable for routine checking of the corrosion status of the tubing materials time by time (Section 7-3).

LPR is not suitable for stainless steel which is susceptible to pitting and not uniform corrosion.

The stainless steel probe needs more investigation due to the difficult of the prediction of the localized corrosion.

# 9 References

Acuña, I.A., Monsegue, A., Brill, T.M., Graven, H., Mulders, F., Le Calvez, J.-L., Nichols, A., Bermudez, F.Z., 2010. Scanning for downhole corrosion, Schlumberger Oilfield Review.

Allen, T., Roberts, A., 1978. Production Operations, Tulsa. ed. Oil and Gas Consultants, Inc.

Arts, R., Winthaegen, P., 2005. Monitoring options for CO2 storage, in: Carbon Dioxide Capture for Storage in Deep Geologic Formations. Elsevier Ltd., pp. 1001–1013.

Cerruti, S., 1998. An Overview of Corrosion Resistant Alloy Steel Selection and Requirements for Oil and Gas Industry. AGIP, Italy.

Choi, Y.-S., Nesić, S., Young, D., 2010. Effect of Impurities on the Corrosion Behavior of Carbon Steel in Supercritical CO2-Water Environments, in: CORROSION 2010, Paper No. 10196. NACE International, Houston.

Choi, Y.-S., Young, D., Nešić, S., Gray, L.G.S., 2013. Wellbore integrity and corrosion of carbon steel in CO2 geologic storage environments: A literature review. Int. J. Greenh. Gas Control 16, S70–S77.

Dugstad, A., Halgorzata, M., Morland, B., 2011. Corrosion in dense phase CO2 pipelines - state of the art, in: Paper No. 4954. Presented at the Eurocorr 2011, Stockholm, Sweden.

El Alami, H., Augustin, C., Orlans, B., Servier, J.J., 2011. Carbon Capture and Storage projects: material integrity for CO2 injection and storage, in: Paper No. 4741. Presented at the Eurocorr 2011, Stockholm, Sweden.

Fontana, M.G., 1986. Corrosion Engineering. McGraw-Hill.

Homborg, A.M., Tinga, T., Zhang, X., van Westing, E.P.M., Oonincx, P.J., de Wit, J.H.W., Mol, J.M.C., 2012. Time–frequency methods for trend removal in electrochemical noise data. Electrochimica Acta 70, 199–209.

Homborg, A.M., van Westing, E.P.M., Tinga, T., Zhang, X., Oonincx, P.J., Ferrari, G.M., de Wit, J.H.W., Mol, J.M.C., 2013. Novel time–frequency characterization of electrochemical noise data in corrosion studies using Hilbert spectra. Corros. Sci. 66, 97–110.

Jaske, C., Beavers, J., Thompson, N., 1995. Improving Plant Reliability Through Corrosion Monitoring. Presented at the Fourth International Conference on Process Plant Reliability, Houston, Texas.

Kermen, E., Meekes, S., 2013. CATO-2 Deliverable WP3.4-D17 Monitoring Strategies for Inaccessible/Abandoned Wells. The Netherlands.

Kolenberg, Y., van Heekeren, H., Boersma, K., Gutierrez-Neri, M., 2012. CATO-2 Deliverable WP3.4-D15 Evaluation of current logging tools and industry practices for material selection and repairs. Netherlands.

Nagelhout, A., Defrancq, J., Kolthof, W., Degener, F., Smit, W., 2009. SodM Report on CSS and Well Integrity: Well Construction Materials in a CO2 Environment. IF-WEP.

Pfennig, A., Bäßler, R., 2009. Effect of CO2 on the stability of steels with 1% and 13% Cr in saline water. Corros. Sci. 51, 931–940.

Rohrback Cosasco Systems, n.d.

Schlumberger, 2009. EM Pipe Scanner.

Seiersten, M., 2001. Materials Selection for Separation, Transportation and Disposal of CO2, in: CORROSION 2001, Paper No. 01042. NACE International, Houston.

Seiersten, M., Kongshaug, K.O., 2005. Materials selection for capture, compression, transport and injection of CO2, in: Carbon Dioxide Capture for Storage in Deep Geologic Formations. Elsevier Ltd., pp. 937–953.

Stern, M., Geary, A.L., 1957. Electrochemical Polarization 1. Theoretical analysis of the shape and polarization curves. J. Electrochem. Soc. 104, 56–63.

USEPA, 1987. Technical Assistance Document: Corrosion, Its Detection and Control in Injection Wells ( No. EPA 570/9-87-002).

USEPA, 2012. Underground Injection Control (UIC) Program Class VI Well Construction Guidance.

USEPA, 2013. Underground Injection Control (UIC) Program Class VI Well Testing and Monitoring Guidance.

Weatherford, 2010a. Multi-Sensor Caliper (MSC TM) Tool.

Weatherford, 2010b. Casing Imaging Tool (CIT).

Weatherford, 2010c. Ultrasonic Radial Scanner (URS).

Zhang, X., Akemu, A., 2010. CATO-2 Deliverable WP3.4-D05 Progress report: Specifications and design criteria for innovatiove corrosion monitoring and (downhole) sensor systems.

Zhang, X., Zevenbergen, J., Benedictus, T., 2013. Corrosion Studies on Casing Steel in CO2 Storage Environments. Energy Procedia 37, 5816–5822.